action of ADAMB should markedly reduce the effective dose for once or twice daily administration without any manipulation of the drug formulation to extend its duration of action.

Although μ-opioid receptor agonists are very important for the control of pain in the clinical setting, these drugs have several undesirable side effects, including respiratory depression,[25] constipation,[26] and dependence.[27] Some of these effects are thought to be related to one of the μ-receptor subtypes, either the μ_1- or the μ_2-receptor. For example, opioid analgesia has been suggested to be mediated by the μ_1-receptor, whereas the μ_2-receptor seems to be involved in respiratory depression and effects on gastrointestinal transit.[28] TAPA and DAS-DER are known to have a high affinity for the μ_1-opioid receptor subtype since their antinociceptive activity is strongly antagonized by pretreatment with naloxonazine, an irreversible μ_1-opioid receptor antagonist.[29] Therefore, it can be expected that these compounds may show a substantial reduction in the adverse effects of μ-opioid peptides that are elicited through the μ_2-opioid receptor. This seems to be the case for ADAMB. The antinociceptive activity of sc ADAMB in mice was markedly attenuated by pretreatment with naloxonazine, a selective μ_1-antagonist, and the same level of attenuation was achieved as that seen with nonselective naloxone. In contrast, morphine was partially antagonized by naloxonazine but was completely antagonized by naloxone. These results imply that ADAMB has a strong antinociceptive action mainly through interaction with the μ_1-opioid receptor subtype. In fact, we have obtained preliminary experimental results in animals to support our assumption that ADAMB inherits promising characteristics as an analgesic from its parent compounds. Less constipation in comparison to that caused by morphine and negligible psychological dependence were observed in mice, as well as low cross-tolerance for morphine (the details will be reported elsewhere).

In conclusion, ADAMB was synthesized based on the structures of several dermorphin tetrapeptide analogues and showed more potent antinociceptive activity than morphine in the mouse tail pressure test after sc and po administration. This strong and long-lasting activity after oral administration may qualify ADAMB as a candidate for the development as a new analgesic. Further investigations are now underway to confirm whether ADAMB also avoids side effects owing to its μ_1-subtype selective agonism.

Experimental Section

Commercial N^{α}-Fmoc-protected amino acids, N^{α}-Boc-protected amino acids, trifluoroacetic acid (TFA), WSCI·HCl, and HOBt were obtained from Peptide Institute, Inc., Osaka, Japan. HBTU was purchased from Calbiochem-Novabiochem Japan Ltd., Tokyo, Japan. Wang resin (100–200 mesh, 0.37 mmol/g) was obtained from Watanabe Chemical Industries Ltd., Hiroshima, Japan, and 1*H*-pyrazole-1-carboxamidine hydrochloride was purchased from Aldrich Chemicals, WI. Fmoc-MeβAla-OH was prepared according to the reported method[30] with Fmoc-OSu and MeβAla. Boc-D-Arg(Cbz$_2$)OH was prepared according to the procedure reported by Jetten.[31] Thin-layer chromatography was performed on silica plates (0.25 mm; Merck, 60 F_{254}). Flash column chromatography for the intermediates of solution phase synthesis was performed using Merck silica gel 60 (230–400 mesh). Purification of the final products was achieved by the flush chromatography using a C-18 reverse phase silica gel Chromatorex DM1020T, Fuji Silysia Chemical Ltd., Aichi, Japan, eluted by a stepwise gradient of acetonitrile (starting from 1% and stepwise gradient by 2%) in 0.1 M acetic acid. Analytical HPLC was on a reverse phase Nucleosil 5C$_{18}$ column (4.6 mm × 150 mm) in a Shimadzu LC-10A HPLC system. The products were analyzed with the two different eluting systems; A: a linear gradient of 10–70% acetonitrile in 0.1% aqueous TFA over 15 min; B: an isocratic elution with 12% acetonitrile in 0.1% aqueous TFA over 30 min. The flow rate was 1 mL/min, and the chromatogram was recorded by UV detection at 230 and 280 nm. ^{1}H NMR spectra were recorded with a JEOL AL-300 (300 MHz) spectrometer, using tetramethylsilane (TMS) as an internal standard. HRMS were obtained with JEOL mass spectrometer model JMS-700.

Solid Phase Synthesis of N^{α}-Amidino-Tyr-D-Arg-Phe-MeβAla-OH (ADAMB). The peptide was synthesized using an N^{α}-Fmoc strategy and Wang resin. The peptides were carried using a Perkin-Elmer model 430A automated synthesizer on a 0.25 mmol scale. Fmoc-D-Arg(Pmc)OH and Fmoc-Tyr(*t*-Bu) were used for the side chain protection. N^{α}-Fmoc-protected amino acids (4 equiv) were added sequentially, using HBTU with HOBt as coupling reagents in NMP. After the peptide assembly was completed, the Fmoc group was removed from the Fmoc-Tyr(*t*-Bu)-D-Arg(Pmc)Phe-MeβAla-Aliko resin, and the peptide resin was mixed with 1*H*-pyrazole-1-caboxamidine hydrochloride (0.99 g, 6.75 mmol) and diisopropylethylamine (1.29 mL, 7.40 mmol) in DMF (6 mL) and agitated at room temperature overnight. The peptides were cleaved using standard techniques and a cleavage mixture of 90% TFA, 5% anisole, 2.5% methyl sulfide, and 2.5% 1,2-ethandithiol. The aqueous solution of the crude products was neutralized with $NaHCO_3$ and then purified by the method shown above to give the desired compound (60 mg, 39%) as acetic acid salts after lyophilization. $[\alpha]_{25}^{D}$ +28.8° (*c* 0.58, 1 M AcOH). ^{1}H NMR (CD_3OD, 300 MHz): δ 7.23 (m, 5H), 7.05 (dd, J = 8.4, 2.4 Hz, 2H), 6.72 (d, J = 8.4 Hz, 2H), 5.17 (t, J = 7.2 Hz, 1H), 4.41 (m, 1H), 4.26 (m, 1H), 3.59 (m, 1H), 3.45 (m, 1H), 3.10–2.85 (m, 6H), 2.88 (s, 2H), 2.85 (s, 1H), 2.35 (m, 2H), 1.50 (br m, 2H), 1.23 (m, 2H). FAB-HRMS: calcd for $C_{29}H_{42}N_9O_6$ [M + 1]$^+$, 612.3258; found, 612.3233.

Solution Phase Synthesis of ADAMB. Boc-Phe-MeβAla-OBzl. To a stirred suspension of H-MeβAla-OBzl·*p*-TsOH (8.04 g, 22.0 mmol) in EtOAc (20 mL), Boc-Phe-OH (5.31 g, 20.0 mmol), HOBt (2.97 g, 22.0 mmol), and Et_3N (3.07 mL, 22.0 mmol) were added at −10 °C. Then, WSCI·HCl (4.60 g, 24.0 mmol) was added to the solution. The mixture was stirred for 30 min at the same temperature and overnight at room temperature. The reaction mixture was washed with 1 N HCl, saturated $NaHCO_3$, and brine. The organic phase was dried over $MgSO_4$, filtered, and evaporated in vacuo to give colorless oil (8.45 g, 95.9%). $[\alpha]_{25}^{D}$ +7.2° (*c* 1.05, DMF). ^{1}H NMR ($CDCl_3$, 300 MHz): δ 7.50–7.12 (m, 10H), 5.38 (t, J = 8.7 Hz, 1H), 5.10 (s, 2H), 4.77 (dt, J = 15, 7.5 Hz, 1H), 3.63 (dt, J = 14, 6.6 Hz, 0.67H), 3.46 (dt, J = 6.9, 6.6 Hz, 1H), 3.42 (m, 0.33H), 2.94 (dd, J = 8.1, 3.0 Hz, 2H), 2.81 (s, 1H), 2.67 (s, 2H), 2.53 (dt, J = 13, 6.6 Hz, 1H), 2.42 (m, 0.67H), 2.04 (m, 0.33H), 1.40 (s, 9H). FAB-HRMS: calcd for $C_{25}H_{33}N_2O_5$ [M + 1]$^+$, 441.2389; found, 441.2391.

Boc-D-Arg(Cbz$_2$)Phe-MeβAla-OBzl. Boc-Phe-MeβAla-OBzl (6.54 g, 14.8 mmol) was dissolved into 4 N HCl/EtOAc (20 mL) and stirred for 30 min at room temperature. Et_2O and hexane were added, and the precipitated material was separated by decantation. The residual gum was dissolved in DMF (30 mL) and neutralized with Et_3N at 0 °C. Boc-D-Arg(Cbz$_2$)OH (7.60 g, 14.0 mmol) and HOBt (1.89 g, 14.0 mmol) were added to the solution, and Et_3N (2.10 mL, 15.0 mmol) was added. Then, WSCI·HCl (3.22 g, 16.8 mmol) was added to the solution at −10 °C. This mixture was stirred for 30 min at −10 °C and overnight at 4 °C. The reaction mixture was diluted with EtOAc (150 mL) and washed with 1 N HCl, 10% Na_2CO_3, and brine. The organic phase was dried over $MgSO_4$, filtered, and evaporated in vacuo. The residue was solidified from hexane

to give the tripeptide as white amorphous (11.7 g, 96.7%). $[\alpha]_{25}^{D}$ +3.9° (*c* 1.00, DMF). ^{1}H NMR ($CDCl_3$, 300 MHz): δ 9.45 (br s, 1H), 9.26 (br s, 1H), 7.43–7.04 (m, 20H), 6.90 (br t, *J* = 7.0 Hz, 1H), 5.46–4.97 (m, 6H), 5.23 (s, 2H), 5.10 (s, 2H), 4.15 (m, 1H), 3.97 (m, 1H), 3.92 (m, 1H), 3.62(dt, *J* = 14, 6.9 Hz, 0.67H), 3.40 (m, 0.33H), 3.50 (m, 1H), 2.86 (br d, *J* = 7.5 Hz, 2H), 2.78 (s, 1H), 2.65 (s, 2H), 2.49 (dt, *J* = 6.9, 3.0 Hz, 1H), 2.39 (m, 0.67H), 2.18 (m, 0.33H), 1.92 (m, 1H), 1.70 (m, 1H), 1.56 (m, 2H), 1.41 (s, 9H). FAB-MS 865 $[M + 1]^+$. Anal. ($C_{47}H_{56}N_6O_{10}$) C, H, N.

Boc-Tyr(Bzl)-D-Arg(Cbz$_2$)Phe-MeβAla-OBzl (7). Boc-D-Arg(Cbz$_2$)Phe-MeβAla-OBzl (4.76 g, 5.50 mmol) was dissolved into 4 N HCl/EtOAc (20 mL) and stirred for 25 min at room temperature. Et_2O was added to the solution, and the precipitated solid was separated by filtration to give the Boc-removed tripeptide quantitatively. This amine component, Boc-Tyr(Bzl)-OH (1.86 g, 5.00 mmol), and HOBt (743 mg, 5.50 mmol) were dissolved in DMF (10 mL), and WSCI·HCl (1.15 g, 6.00 mmol) was added to the solution at −8 °C. The pH of the solution was adjusted to 5 with Et_3N (1.35 mL). This mixture was stirred for 30 min at −8 °C and overnight at 4 °C. The reaction mixture was diluted with EtOAc (100 mL) and washed with 10% citric acid, saturated $NaHCO_3$, and brine. The organic phase was dried over $MgSO_4$, filtered, and evaporated in vacuo. The residue was solidified from EtOAc and hexane to give white amorphous (4.76 g, 85.8%). $[\alpha]_{25}^{D}$ −3.2° (c 1.04, DMF). ^{1}H NMR ($CDCl_3$, 300 MHz): δ 9.49 (br s, 1H), 9.29 (br s, 1H), 7.60–7.00 (m, 26H), 7.00 (d, *J* = 8.7 Hz, 2H), 6.81 (d, *J* = 8.7 Hz, 2H), 6.79 (br s, 1H), 5.29–4.88 (m, 6H), 5.08 (s, 2H), 4.95 (s, 2H), 4.49 (m, 1H), 4.29 (m, 1H), 3.80 (m, 1H), 3.67 (m, 1H), 3.42 (m, 1H), 3.03–2.79 (m, 5H), 2.76 (s, 1H), 2.65 (s, 2H), 2.46 (br t, *J* = 7.5 Hz, 1.33H), 2.40 (m, 0.67H), 2.16 (m, 2H), 1.54 (m, 2H), 1.36 (s, 9H). FAB-MS 1119 $[M + 1]^+$. Anal. ($C_{63}H_{71}N_7O_{12}$) C, H, N.

N$^{\alpha}$-(N,N'-Bis-benzyloxycarbonyl)amidino-Tyr(Bzl)-D-Arg(Cbz$_2$)Phe-MeβAla-OBzl (8). Tetrapeptide 7 (2.43 g, 2.20 mmol) was dissolved in 4 N HCl/dioxane (20 mL) at −8 °C and stirred for 30 min at room temperature. Et_2O (80 mL) was added to the solution, and the precipitated oil was separated by decantation. The residue was solidified from Et_2O (40 mL). The solid was collected by filtration and dried under a reduced pressure to give Boc-removed tetrapeptide (2.23 g, 97.4%) as a white powder. This amine hydrochloride (1.04 g, 1.00 mmol) and (benzyloxycarbonylimino-pyrazol-1-yl-methyl)carbamic acid benzyl ester (416 mg, 1.10 mmol) were dissolved in DMF (2 mL). The pH of the solution was adjusted to 8 with Et_3N (210 μL) at 0 °C. The mixture was stirred for 6 h at room temperature, and Et_3N (50 μL) was added in the middle of the reaction to keep the pH 8. The reaction mixture was poured into 10% citric acid (15 mL), and the precipitated oil was extracted with EtOAc (40 mL). The EtOAc solution was washed with brine, dried over $MgSO_4$, filtered, and evaporated in vacuo. The residual oil was purified by flush chromatography eluted with $CHCl_3$:MeOH (100:1) followed by precipitation from Et_2O to give white amorphous powder (0.93 g, 71.0%). $[\alpha]_{25}^{D}$ +8.9° (*c* 1.01, DMF). ^{1}H NMR ($CDCl_3$, 300 MHz): δ 11.50 (s, 1H), 9.48 (br s, 1H), 9.26 (br s, 1H), 8.81 (t, *J* = 7.5 Hz, 1H), 7.47–7.09 (m, 35H), 7.06 (d, *J* = 8.4 Hz, 2H), 6.87 (d, *J* = 8.1 Hz, 1H), 6.81 (d, *J* = 8.4 Hz, 2H), 5.23–4.86 (m, 14H), 4.76 (dt, *J* = 7.2, 7.2 Hz, 1H), 4.42 (dt, *J* = 7.0, 7.0 Hz, 1H), 3.59 (m, 1H), 3.70 (m, 1H), 3.59 (m, 1H), 3.27 (m, 1H), 2.99 (br t, *J* = 6.0, 2H), 2.80 (br d, *J* = 7.2 Hz, 2H), 2.70 (s, 1H), 2.57 (s, 2H), 2.42 (t, *J* = 7.2 Hz, 1.33H), 2.35 (m, 0.67H), 1.99 (br s, 2H), 1.49 (m, 2H). FAB-MS 1329 $[M + 1]^+$. Anal. ($C_{75}H_{77}N_9O_{14}$) C, H, N.

N$^{\alpha}$-Amidino-Tyr-D-Arg-Phe-MeβAla-OH (ADAMB). To the solution of protected tetrapeptide 8 (657 mg, 0.50 mmol) in AcOH (10 mL) was added 10% Pd–C (50% wet). This solution was vigorously stirred under H_2 atmosphere for 4 h at room temperature. The catalyst was removed by filtration, and the filtrate was concentrated in vacuo. The residue was precipitated from Et_2O to give a white powder (0.30 g, 91.2%) as acetate salt.

N$^{\alpha}$-Amidino-Tyr-D-Arg-Phe-βAla-OH (1). The same solid phase procedure for the synthesis of ADAMB was employed, but Fmoc-βAla-Wang resin was used instead of Fmoc-MeβAla-Wang resin as a starting material to give 1 as a white powder (60 mg, 43%). $[\alpha]_{25}^{D}$ +20.5° (*c* 1.11, 1M AcOH). ^{1}H NMR (CD_3OD, 300 MHz): δ 7.24 (m, 5H), 7.06 (d, *J* = 8.4 Hz, 2H), 6.70 (d, *J* = 8.4 Hz, 2H), 4.58 (dd, *J* = 11, 4.2 Hz, 1H), 4.36 (t, *J* = 7.2 Hz, 1H), 3.97 (t, *J* = 7.2 Hz, 1H), 3.57–3.32 (m, 3H), 3.07–2.83 (m, 4H), 2.76 (dd, *J* = 14, 11 Hz, 1H), 2.38 (t, *J* = 6.3 Hz, 2H), 1.41 (m, 2H), 1.14 (m, 1H), 0.93 (m, 1H). FAB-HRMS: calcd for $C_{28}H_{40}N_9O_6$ $[M + 1]^+$, 598.3102; found, 598.3125.

N$^{\alpha}$-Amidino-Tyr-D-Arg-Phe-Sar-OH (2). The same solid phase procedure for the synthesis of ADAMB was employed, but Fmoc-Sar-Wang resin was used instead of Fmoc-MeβAla-Wang resin as a starting material to give 2 as a white powder (63 mg, 42%). $[\alpha]_{25}^{D}$ +26.5° (*c* 0.35, 1M AcOH). ^{1}H NMR (CD_3OD, 300 MHz): δ 7.17 (m, 5H), 7.01 (d, *J* = 8.1 Hz, 2H), 6.67 (d, *J* = 8.1 Hz, 2H), 5.08 (t, *J* = 6.3 Hz, 1H), 4.35 (br s, 1H), 4.19 (m, 1H), 3.98 (t, *J* = 17 Hz, 1H), 3.83 (d, *J* = 18 Hz, 1H), 3.67 (m, 1H), 3.14–2.73 (m, 9H), 1.51 (m, 1H), 1.40 (m, 1H), 1.16 (m, 2H). FAB-HRMS: calcd for $C_{28}H_{40}N_9O_6$ $[M + 1]^+$, 598.3102; found, 598.3108.

H-Tyr-D-Arg-Phe-MeβAla-OH (3). The same solid phase procedure for the synthesis of ADAMB was employed, but the amidination process was skipped to give 3 as a white powder (76 mg, 53%). $[\alpha]_{25}^{D}$ +47.4° (*c* 0.84, 1 M AcOH). ^{1}H NMR (CD_3OD, 300 MHz): δ 7.25 (m, 5H), 7.11 (d, *J* = 8.4 Hz, 2H), 6.74 (d, *J* = 8.4 Hz, 2H), 5.12 (t, *J* = 7.2 Hz, 1H), 4.22 (m, 1H), 4.09 (m, 1H), 3.53 (br t, *J* = 7.2 Hz, 2H), 3.17–2.89 (m, 6H), 2.89 (s, 2H), 2.85 (s, 1H), 2.42 (m, 2H), 1.42 (m, 2H), 1.18 (m, 2H). FAB-HRMS: calcd for $C_{28}H_{40}N_7O_6$ $[M + 1]^+$, 570.3040; found, 570.3021.

H-MeTyr-D-Arg-Phe-MeβAla-OH (4). The same solid phase procedure for the synthesis of ADAMB was employed, but Fmoc-MeTyr(*t*-Bu)OH was used instead of Fmoc-Tyr(*t*-Bu)OH, and the amidination process was skipped to give 4 as a white powder (80 mg, 55%). $[\alpha]_{23}^{D}$ +44.4° (*c* 1.01, 1M AcOH). ^{1}H NMR (CD_3OD, 300 MHz): δ 7.21 (m, 5H), 7.00 (d, *J* = 8.4 Hz, 2H), 6.70 (dd, *J* = 8.4, 2.7 Hz, 2H), 5.18 (t, *J* = 7.2 Hz, 0.5H), 5.00 (t, *J* = 7.5 Hz, 0.5H), 4.24 (dt, *J* = 6.0, 6.0 Hz, 1H), 3.63 (br m, 1H), 3.42 (br m, 2H), 3.10–2.63 (m, 6H), 2.87 (d, *J* = 6.3 Hz, 3H), 2.38 (br m, 2H), 2.29 (d, *J* = 6.6 Hz, 3H), 1.43 (br m, 2H), 1.09 (m, 2H). FAB-HRMS: calcd for $C_{29}H_{42}N_7O_6$ $[M + 1]^+$, 584.3197; found, 584.3203.

Me$_2$Tyr-D-Arg-Phe-MeβAla-OH (5). The same solid phase procedure for the synthesis of ADAMB was employed, but Me$_2$Tyr(*t*-Bu)OH was used instead of Fmoc-Tyr(*t*-Bu)OH, and the amidination process was skipped to give 5 as a white powder (68 mg, 45%). $[\alpha]_{23}^{D}$ +44.4° (*c* 1.08, 1 M AcOH). ^{1}H NMR (CD_3OD, 300 MHz): δ 7.21 (m, 5H), 7.00 (d, *J* = 8.4 Hz, 2H), 6.70 (dd, *J* = 8.4, 1.5 Hz, 2H), 5.15 (t, *J* = 6.9 Hz, 0.5H), 4.99 (t, *J* = 7.5 Hz, 0.5H), 4.14 (m, 1H), 3.54 (m, 1H), 3.43 (m, 2H), 3.10–2.80 (m, 6H), 2.89 (s, 2H), 2.85 (s, 1H), 2.53 (s, 3H), 2.51 (s, 3H), 2.35 (br m, 2H), 1.38 (m, 1H), 1.24 (m, 1H), 0.95 (m, 2H). FAB-HRMS: calcd for $C_{30}H_{44}N_7O_6$ $[M + 1]^+$, 598.3353; found, 598.3321.

N$^{\alpha}$-Ac-Tyr-D-Arg-Phe-βAla-OH (6). The same solid phase procedure for the synthesis of 1 was employed, but *N*-terminal was acetylated with acetic anhydride instead of amidination to give 6 as a white powder (84 mg, 56%). $[\alpha]_{25}^{D}$ +30.6° (*c* 0.87, 1M AcOH). ^{1}H NMR (DMSO-d_6, 300 MHz): δ 9.73 (t, 5.1 Hz, 1H), 8.29 (m, 1H), 8.09 (d, *J* = 8.4 Hz, 1H), 7.89 (t, *J* = 5.1 Hz, 1H),7.01 (m, 6H), 7.00 (d, *J* = 8.1 Hz, 2H), 6.64 (d, *J* = 8.1 Hz, 2H), 4.38 (dt, *J* = 7.2, 7.2 Hz, 1H), 4.29 (m, 1H), 4.03 (dd, *J* = 14, 7.5 Hz, 1H), 3.30–3.05 (m, 3H), 2.96 (br d, *J* = 3.9 Hz, 2H), 2.98–2.60 (m, 3H), 2.14 (m, 2H), 1.77 (s, 3H), 1.57 (m, 1H), 1.42 (m, 1H), 1.22 (m, 2H). FAB-HRMS: calcd for $C_{29}H_{40}N_7O_7$ $[M + 1]^+$, 598.2989; found, 598.2967.

Binding Assays. Synaptosomal fractions were prepared from mice spinal cord and guinea pig cerebella according to the method of Chang et al.[32] Briefly, spinal cord or cerebella was homogenized in a 0.32 M sucrose solution at 0 °C and centrifuged at 6000*g* for 15 min. The supernatant was centri-

fuged at 40 000*g* for 30 min, and the pellets were homogenized in 5 mM Tris-HCl buffer (pH 7.4) at 0 °C. The suspension was centrifuged at 6000*g* for 15 min. The supernatant was then centrifuged twice at 40 000*g* for 30 min each. After the second centrifugation, the membranes were resuspended in 50 mM Tris-HCl buffer (pH 7.4).

[^{3}H]DAMGO, [^{3}H]deltorphin-II, and [^{3}H]U-69593 were used for the determination of relative affinities for μ-, δ-, and κ-receptors, respectively. Binding assays were carried out by incubating an aliquot of the membrane fraction (250 μg for [^{3}H]DAMGO, 350 μg for [^{3}H]deltorphin-II, and 180 μg for [^{3}H]U-69593) containing protease inhibitors and the labeled ligand (3 nM for [^{3}H]DAMGO or [^{3}H]deltorphin-II, and 2 nM for [^{3}H]U-69593) in 50 mM Tris-HCl buffer (pH 7.4). After 60 min at 25 °C, the reaction mixture was filtered over a Whatman GF/B filter soaked with 0.1% polyethyleneimine and the filter was washed twice with cold Tris-HCl buffer. Filters were counted in a liquid scintillation counter after overnight extraction with liquid scintillation fluid (3 mL). Specific binding was determined from the differences between total binding and that in the presence of excess (10 μM) unlabeled ligand. K_d and B_{max} values were obtained using Scatchard analysis.

Antinociceptive Assay. Male mice of ddY strain weighing 10–32 g were used in the experiment. They were purchased from Japan SLC Inc. (Shizuoka, Japan) and housed in cages of 5–6 animals, matched for weight, and placed in a colony room. Animals were given standard food (MM-3, Japan SLC Inc.) and tap water ad libitum in an air-conditioned room at 23 ± 2 °C and 50 ± 10% relative humidity with a standard 12 h light–dark cycle (lights on 6:00–18:00). The tail pressure test was performed according to the reported method by Sakurada et al.[33] with a slight modification. Thus, mechanical pressure was applied to the base of the tail at a rate of 32 g/sec using an automated tail pressure unit (Ugo Basile, Italy). Biting or struggling behavior in mice was used as an indication of response threshold, and only mice responding behaviorally to a tail pressure of 100–300 g were selected for this experiment. The trials were terminated at the level of 500 g to prevent tail tissue damage. The mean ± SEM of the pressure level was plotted. To obtain the response curve, the dose was plotted against percentage of MPE (% MPE = $(P_2 - P_1/500 - P_1) \times 100$, where P_1 is the response pressure before drug administration (g) and P_2 is the response pressure after drug administration (g). In the hot plate test,[34] the animals were placed on a 55 °C hot plate (Ugo Basil, model-DS37) surrounded by a glass tube (ϕ14 × 13 H cm), and the latency of either a jump or a hindpaw lick was measured. Prior to drug administration, the nociceptive response of each mouse was measured and mice showing the response in 10–20 s after placement were chosen for the test. A cutoff time of 40 s was used to minimize tissue damage. The peptides administered were dissolved in saline solution (Fuso Chemical Industries, Osaka, Japan). Saline solution was used as the control. ED_{50} vales were obtained by the method of Litchfield and Wilcoxon.[35]

References

(1) Hughes, J.; Smith, T. W.; Kosterlitz, H. W.; Fothergill, L. A.; Morgan, B. A.; Morris, H. R. Identification of Two Related Pentapeptides from the Brain with Potent Opiate Agonist Activity. *Nature* 1975, *258*, 577–579.

(2) Roques, B. P.; Noble, F.; Fournie-Zaluski, M.-C. Endogenous Opioid Peptides and Analgesia. In *Opioids Pain Control*; Stein, C., Ed.: Cambridge University Press: Cambridge, 1999; pp 21–45.

(3) Ahmedazi, S. New Approaches to Pain Control in Patients with Cancer. *Eur. J. Cancer* 1997, *33* (Suppl. 6), S8–S14.

(4) Montecucchi, P. C.; De Castiglione, R.; Erspamer, V. Identification of Dermorphin and 6-Hyp-Dermorphin in Skin Extracts of the Brazilian Frog *Phyllomedusa Rhodei*. *Int. J. Pept. Protein Res.* 1981, *17*, 316–321.

(5) Erspamer, V.; Melchiorri, P.; Broccardo, M.; Erspamer, G. F.; Falaschi, P.; Improta, G.; Negri, L.; Renda, T. The Brain-Gut-Skin Triangle. New Peptides. *Peptides* 1981, *2* (Suppl. 2), 7–16.

(6) Broccardo, M.; Erspamer, V.; Erspamer, G. F.; Improta, G.; Linari, G.; Melchiorri, P.; Montecucchi, P. C. Pharmacological Data on Dermorphins, a New Class of Potent Opioid Peptides from Amphibian Skin. *Br. J. Pharmacol.* 1981, *73*, 625–631.

(7) Sato, T.; Sakurada, S.; Sakurada, T.; Furuta, S.; Chaki, K.; Kisara, K.; Sasaki, Y.; Suzuki, K. Opioid Activities of D-Arg^2-Substituted Tetrapeptides. *J. Pharmacol. Exp. Ther.* 1987, *242*, 654–659.

(8) de Castiglione, R.; Rossi, A. C. Structure–Activity Relationships of Dermorphin Synthetic Analogues. *Peptides* 1985, *6* (Suppl. 3), 117–125.

(9) Takagi, H.; Shiomi, H.; Ueda, H.; Amano, H. Morphine-Like Analgesia by a New Dipeptide, L-Tyrosyl-L-Arginine (Kyotorphin) and its Analogue. *Eur. J. Pharmacol.* 1979, *55*, 109–111.

(10) Schiller, P. W.; Nguyen, T. M.-D.; Chung, N. N.; Lemieux, C. Dermorphin Analogues Carrying an Increased Positive Net Charge in their "Message" Domain Display Extremely High μ-Opioid Receptor Selectivity. *J. Med. Chem.* 1989, *32*, 698–703.

(11) Salvadori, S.; Marastoni, M.; Tomatis, R. Opioid Peptides. Structure–Activity Relationships in Dermorphin Tetrapeptides. *Il Farmaco Ed. Sci.* 1982, *37*, 514–518.

(12) Sakurada, S.; Murayama, K.; Nakano, M.; Hongo, K.; Takeshima, S.; Take, N. Peptide Derivatives. PCT Int. Appl. WO 9524421, 1995; *Chem. Abstr.* 1996, *124*, 146854.

(13) Sasaki, Y.; Matsui, M.; Taguchi, M.; Suzuki, K.; Sakurada, S.; Sato, T.; Sakurada, T.; Kisara, K. D-Arg^2-Dermorphin Tetrapeptide Analogues. A Potent and Long-Lasting Analgesic Activity after Subcutaneous Administration. *Biochem. Biophys. Res. Commun.* 1984, *120*, 214–218.

(14) Paakkari, P.; Paakkari, I.; Bonhof, S.; Feuerstein, G.; Sirén, A.-L. Dermorphin analogue Tyr-D-Arg^2-Phe-Sarcosine-Induced Opioid Analgesia and Respiratory Stimulation. The Role of Mu$_1$-receptors? *J. Pharmacol. Exp. Ther.* 1993, *266*, 544–550.

(15) Sato, T.; Takahashi, N.; Tan-No, K.; Kisara, K.; Sakurada, T.; Sakurada, S. Comparison of Opioid Activity Between a *N*-Terminal Tetrapeptide Analogue of Dermorphin, H-Tyr-D-Arg-Phe-β-Ala-OH and Morphine. *Methods Find Exp. Clin. Pharmacol.* 1998, *20*, 581–586.

(16) Chaki, K.; Kawamura, S.; Kisara, K.; Sakurada, S.; Sakurada, T.; Sasaki, Y.; Sato, T.; Suzuki, K. Antinociception and Physical Dependence Produced by [D-Arg^2]Dermorphin Tetrapeptide Analogues and Morphine in Rats. *Br. J. Pharmacol.* 1988, *95*, 15–22.

(17) Chaki, K.; Sakurada, S.; Sakurada, T.; Sato, T.; Kawamura, S.; Kisara, K.; Sasaki, Y.; Suzuki, K. A New Class Opioid Peptide, [D-Arg^2, β-Ala^4]Dermorphin Tetrapeptide. Physical Dependence Liability in Mice. *Neuropeptides* 1989, *13*, 83–88.

(18) Fields, G. B.; Noble, R. L. Solid Phase Peptide Synthesis Utilizing 9-Fluorenylmethoxycarbonyl Amino Acids. *Int. J. Pept. Protein Res.* 1990, *35*, 161–214.

(19) Bernatowicz, M. S.; Wu, Y.; Matsueda, G. R. 1*H*-Pyrazole-1-carboxamidine Hydrochloride. An Attractive Reagent for Guanylation of Amines and Its Application to Peptide Synthesis. *J. Org. Chem.* 1992, *57*, 2497–2502.

(20) Bernatowicz, M. S.; Wu, Y.; Matsueda, G. R. Urethane Protected Derivatives of 1-Guanylpyrazole for the Mild and Efficient Preparation of Guanidines. *Tetrahedron Lett.* 1993, *34*, 3389–3392.

(21) (a) Sakurada, S.; Takeda, S.; Sato, T.; Hayashi, T.; Yuki, M.; Kutsuwa, M.; Tan-No, K.; Sakurada, C.; Kisara, K., Sakurada, T. Selective Antagonism by Naloxonazine of Antinociception by Tyr-D-Arg-Phe-β-Ala, A Novel Dermorphin Analogue with High Affinity at μ-Opioid Receptors. *Eur. J. Pharmacol.* 2000, *395*, 107–112. (b) Upton, N.; Sewell, R. D. E.; Spencer, P. S. J. Analgesic Action of μ- and κ-Opiate Agonists in Rats. *Arch. Int. Pharmacodyn.* 1983, *262*, 199–207. (c) Endoh, T.; Matsuura, H.; Tajima, A.; Izumimoto, N.; Tajima, C.; Suzuki, T.; Saitoh, A.; Suzuki, T.; Narita, M.; Tseng, L.; Nagase, H. Potent Antinociceptive Effects of TRK-820, A Novel κ-Opioid Receptor Agonist. *Life Sci.* 1999, *65*, 1685–1694.

(22) Negri, L.; Melchiorri, P.; Lattanzi, R. Pharmacology of Amphibian Opiate Peptides. *Peptides* 2000, *21*, 1639–1647.

(23) Morley, J. S. Structure–Activity Relationships of Enkephalin-Like Peptides. *Annu. Rev. Pharmacol. Toxicol.* 1980, *20*, 81–110.

(24) Marastoni, M.; Salvadori, S.; Balboni, G.; Borea, P. A.; Marzola, G.; Tomatis, R. Synthesis and Activity Profiles of New Dermorphin-(1–4) Peptide Analogues. *J. Med. Chem.* 1987, *30*, 1538–1542.

(25) Popio, K. A.; Jackson, D. H.; Ross, A. M.; Schreiner, B. F.; Yu, P. N. Hemodynamic and Respiratory Effects of Morphine and Butorphanol. *Clin. Pharmacol. Ther.* 1978, *23*, 281–287.

(26) (a) Stewart, J. J.; Weisbrodt, N. W.; Burks, T. F. Central and Peripheral Actions of Morphine on Intestinal Transit. *J. Pharmacol. Exp. Ther.* 1978, *5*, 547–555. (b) Schulz, R.; Wuster, M.; Herz, A. Centrally and Peripherally Mediated Inhibition of Intestinal Motility by Opioids. *Naunyn Schmiedeberg's Arch Pharmacol.* 1979, *308*, 255–260.
(27) Martin, W. R. Drug Addiction: Morphine, Sedative/Hypnotic and Alcohol Dependence. In *Handbook of Experimental Pharmacology*; Martin, W. R., Ed.; Springer: Berlin, Germany, 1977; Vol. 45, Pt. 1, pp 1–74.
(28) Pasternak, G. W. Parmacological Mechanisms of Opioid Analgesics. *Clin. Neuropharmacol.* 1993, *16*, 1–18.
(29) (a) Pasternak, G. W.; Wood, P. J. Multiple μ Opiate Receptors. *Life Sci.* 1986, *38*, 1889–1898. (b) Ling, G. C. F.; Simantov, S.; Clark, J. A.; Pasternak, G. W. Naloxonazine Actions In Vivo. *Eur. J. Pharmacol.* 1986, *129*, 33–38.
(30) Milton, R. C. de L.; Becker, E.; Milton, S. C. F.; Baxter, J. E. H.; Elsworth, J. F. Improved Purities for Fmoc-Amino Acids from Fmoc-ONSu. *Int. J. Protein Pept. Res.* 1987, *30*, 431–432.
(31) Jetten, M.; Co, A.; Peters, C. A. M.; van Nispen, J. W. F. M.; Ottenheijm, H. C. J. A One-Pot N-Protection of L-Arginine. *Tetrahedron Lett.* 1991, *32*, 6025–6028.
(32) Chang, K. J.; Cuatrecasas, P. Multiple opiate receptors. Enkephalins and Morphine Bind to Receptors of Different Specificity. *J. Biol. Chem.* 1979, *254*, 2610–2618.
(33) Sakurada, S.; Sakurada, T.; Jin, H.; Sato, T.; Kisara, K.; Sasaki, Y.; Suzuki, K. Antinociceptive Activities of Synthetic Dipeptides in Mice. *J. Pharm. Pharmacol.* 1982, *34*, 750–751.
(34) Hammond, D. L.; Stapelfeld, A.; Drower, E. J.; Savage, M. A.; Tam, L.; Mazur, R. H. Antinociception Produced by Oral, Subcutaneous or Intrathecal Administration of SC-39566, an Opioid Dipeptide Arylalkylamide, in the Rodent. *J. Pharmacol. Exp. Ther.* 1994, *268*, 607–615.
(35) Litchfield, J. T.; Wilcoxon, F. A. Simplified Method of Evaluating Dose–Effect Experiments. *J. Pharmacol. Exp. Ther.* 1949, *96*, 99–113.

JM010357T

British Journal of Pharmacology (2002) 137, 1143–1146
www.nature.com/bjp

SPECIAL REPORT

Endomorphin analogues containing D-Pro^2 discriminate different μ-opioid receptor mediated antinociception in mice

*,[1]Shinobu Sakurada, [1]Hiroyuki Watanabe, [1]Takafumi Hayashi, [1]Masayuki Yuhki, [2]Tsutomu Fujimura, [2]Kimie Murayama, [3]Chikai Sakurada & [3]Tsukasa Sakurada

[1]Department of Physiology and Anatomy, Tohoku Pharmaceutical University, 4-4-1 Komatushima, Sendai 981-8558, Japan; [2]Division of Biochemical Analysis, Central Laboratory of Medical Sciences, Juntendo University School of Medicine, 2-1-1 Hongo, Tokyo 113-8421, Japan and [3]Department of Biochemistry, Daiichi College of Pharmaceutical Sciences, 22-1 Tamagawa-cho, Minami-ku, Fukuoka 815-8511, Japan

The antagonistic actions of D-Pro^2-endomorphins on inhibition of the paw withdrawal response by endomorphins were studied in mice. D-Pro^2-endomorphin-1 and D-Pro^2-endomorphin-2, injected intrathecally (i.t.), had no significant effect on the nociceptive thermal threshold alone. When D-Pro^2-endomorphin-1 (0.05–0.1 pmol) was injected simultaneously with i.t. endomorphin-1 (5.0 nmol) or endomorphin-2 (5.0 nmol), antinociception induced by endomoprhin-1 was reduced significantly, whereas endomorphin-2-induced antinociception was not affected by D-Pro^2-endomorphin-1. Antinociception induced by i.t. endomorphin-2 (5.0 nmol) was reduced significantly by its analogue, D-Pro^2-endomorphin-2 (100 pmol), but not by D-Pro^2-endomorphin-1. D-Pro^2-endomorphin-1 also antagonized the antinociceptive effect of i.t. DAMGO, a μ-opioid receptor agonist, whereas D-Pro^2-endomorphin-2 failed to reduce the effect of DAMGO. These results suggest that endomorphin analogues containing D-Pro^2 are able to discriminate the antinociceptive actions of μ_1- and μ_2-opioid receptor agonists at the spinal cord level.
British Journal of Pharmacology (2002) **137**, 1143–1146. doi:10.1038/sj.bjp.0705047

Keywords: D-Pro^2-endomorphin-1; D-Pro^2-endomorphin-2; endomorphins; opioid receptor antagonists; antinociception; intrathecal injection; spinal cord

Abbreviations: CSF, cerebrospinal fluid; i.c.v., intracerebroventricular(ly); i.t., intrathecal(ly); DAMGO, [D-Ala^2, MePhe^4, Gly(ol)^5]enkephalin

Introduction

The newly isolated endogenous opioid tetrapeptides, endomorphin-1 and endomorphin-2, have high affinity and selectivity for μ-opioid receptors (Zadina *et al.*, 1997). Neither endomorphins had appreciable affinity for δ- and κ-opioid receptors. These endomorphins are found in the brain and spinal cord where high densities of μ-opioid receptors occur. Endomorphin-1-like immunoreactivity is more prominent in the brain, whereas endomorphin-2-like immunoreactivity is more prevalent in the spinal cord (Martin-Schild *et al.*, 1999). Thus, endomorphin-1 and -2 are the putative endogenous ligand for the morphine-preferring μ-opioid receptors. Distinct pharmacological properties of endomorphins have been reported in several behavioural experiments in rodents (Zadina *et al.*, 1997; Stone *et al.*, 1997; Sakurada *et al.*, 1999; 2000a; Horvath *et al.*, 1999; Przewlocka *et al.*, 1999). Antinociception induced by endomorphin-1 and endomorphin-2 given intrathecally (i.t.) or intracerebroventricularly (i.c.v.) is selectively blocked by pre-treatment with the μ-opioid receptor antagonists, naloxone or β-funaltrexamine (Zadina *et al.*, 1997; Sakurada *et al.*, 1999; 2000a), indicating that they are mediated by the stimulation of μ-opioid receptors. Furthermore, pre-treatment with the μ_1-opioid receptor antagonist, naloxonazine, attenuates antinociceptive effects induced by i.t. administered endomorphin-2 but not by endomorphin-1, suggesting that endomorphin-2-induced antinociception may be mediated by the stimulation of μ_1-opioid receptors (Sakurada *et al.*, 1999; 2000a). The antinociceptive effect of i.t. DAMGO, a selective μ-opioid agonist, is insensitive to naloxonazine and sensitive to β-funaltrexamine, which binds μ_1- and μ_2-opioid receptors (Pick *et al.*, 1991). The *in vivo* and *in vitro* studies of D-Pro^2-endomorphin-2, an enzyme-resistant analogue of endomorphin-2, have shown that the D-Pro^2 substitution in endomorphin-2 is more potent than endomorphin-2 in significantly increasing tail-flick latencies when injected i.c.v. in rats, since D-Pro^2-endomorphin-2 is totally resistant to the action of dipeptidyl peptidase IV (Shane *et al.*, 1999). In contrast, the pharmacological activity of D-Pro^2-endomorphins is less potent than that of parent tetrapeptides, as drastic loss of activity in the guinea-pig ileum and opioid receptor binding assays occur in the presence of D-Pro^2-endomorphin-1 and D-Pro^2-endomorphin-2 (Paterlini *et al.*, 2000; Okada *et al.*, 2000).

The purpose of the present study is to determine whether D-Pro^2-endomorphins discriminate μ_1- and/or μ_2-opioid receptor mediation of antinociception induced by three different μ-opioid receptor agonists, endomorphin-1, -2 and DAMGO at the spinal cord level.

*Author for correspondence; E-mail: s-sakura@tohoku-pharm.ac.jp

Methods

Adult male ddY mice weighing 22–25 g were housed in a light- and temperature-controlled room (light on 0900 to 2100 h; 23°C) and had free access to food and water. The experiments were performed with the approval of the Committee of Animal Experiments at Tohoku Pharmaceutical University. Endomorphin-1, -2 and D-Pro^2-endomorphins were synthesized in our laboratory. DAMGO was purchased from Sigma (St. Louis, MO, U.S.A.). Endomorphin-1 (5 nmol), endomorphin-2 (5 nmol) and D-Pro^2-endomorphin-1 (0.03–1.0 pmol), D-Pro^2-endomorphin-2 (25–100 pmol) and DAMGO (20 pmol) were dissolved in sterile artificial cerebrospinal fluid (CSF) containing 7.4 g NaCl, 0.19 g KCl, 0.19 g $MgCl_2$, 0.14 g $CaCl_2$ 1000 ml^{-1}. For i.t. administration, a 29-gauge needle connected to Hamilton microsyringe was inserted directly between L5 and L6, and each peptide was administered at a rate of 2 μl 10^{-1}. Endomorphins and DAMGO in combination with D-Pro^2-endomorphins were also co-administered i.t. in a volume of 2 μl.

The antinociceptive activity of opioid peptides against the response to a thermal stimulus was assessed by the mouse paw withdrawal test. Antinociceptive thresholds were determined by an automated tail-flick unit (BM kiki, Tokyo). Mice were adapted to the testing environment for at least 1 h before any stimulation. Each animal was restrained with a soft cloth to reduce visual stimuli, and the radiant heat source was positioned under the glass floor directly beneath the hindpaw. The heat stimulus intensity was determined by the reaction time of the removal of the paw from a source of noxious radiant heat. The intensity of the light beam was adjusted so that baseline reaction time was 2.5–3.5 s. The light beam was focused on the same plantar spot of the hind paw in all animals. To prevent tissue damage, trials were terminated automatically if the mouse did not lift the paw within 10 s. Baseline latencies were determined before experimental treatment for all animals as the mean of two trials. The measurements of hindpaw withdrawal were determined by an experimenter. To prevent experimenter bias, observers were uninformed of the dose of each compound being injected. After determination of pre-drug values, animals were injected. Antinociceptive activity for each animal was calculated with the following equation and represented as per cent of maximum possible effect (% MPE) = (P2 − P1/10 − P1) × 100, where P1 and P2 are pre-drug and post-drug responsive time (in seconds), respectively.

Statistical significance of the data was estimated with a mixed two-factor analysis of variance (ANOVA) followed by Dunnett's multiple comparison test. A level of probability of 0.05 or less was accepted as significant. The ED_{50} or ID_{50} values and their 95% confidence limits (95% CL) for the antinociceptive or antagonistic effect of compounds examined were computed according to our previous report (Sakurada *et al.*, 1999).

Results

The i.t. injection of endomorphin-1 (5 nmol), -2 (5 nmol) and DAMGO (20 pmol) produced a marked antinociceptive effect as assayed by the paw withdrawal test (Figure 1). Endomorphin-1 and -2 at a dose of 5 nmol caused almost equipotent antinociception in intensity and duration. The antinociceptive effect reached a peak at 1 min after injection of both endomorphins, rapidly declined, and returned to the pre-injection level in 20 min. The ED_{50} values for endomorphin-1 and -2 were 0.14 and 0.24 nmol, respectively. The ED_{50} value for i.t. DAMGO was 14.0 pmol at the 5 min peak time of antinociception. These pharmacological properties of endomorphins and DAMGO confirm our previous reported data (Sakurada *et al.*, 2000a). Single injection of D-Pro^2-endomorphin-1 (0.03–1.0 pmol) or D-Pro^2-endomorphin-2 (25–100 pmol) was without affecting the paw withdrawal response (data not shown).

The antagonistic effect of D-Pro^2-endomorphin-1 or D-Pro^2-endomorphin-2 on antinociception induced by i.t. endomorphin-1 and -2 at a dose of 5.0 nmol was examined. As seen in Figure 1, the antinociceptive effect of endomorphin-1 (5 nmol) at 1 or 5 min after i.t. injection was inhibited significantly by co-administration of D-Pro^2-endomorphin-1 (0.08 and 0.1 pmol). The ID_{50} values of D-Pro^2-endomorphin-1 on endomorphin-1-induced antinociception were 0.13 pmol and 0.058 pmol at 1 and 5 min after i.t. co-injection, respectively (Table 1). No further antagonism in antinociception of endomorphin-1 at a dose of 5 nmol was seen by 0.25 or 1.0 pmol of D-Pro^2-endomorphin-1 (Figure 2). The i.t. co-injection of D-Pro^2-endomorphin-2 (25–100 pmol) produced no significant effect on inhibition of the paw withdrawal response induced by i.t. endomorphin-1 (5.0 nmol). Artificial CSF (2 μl) alone, injected i.t., had no apparent effect on inhibition of the paw withdrawal response.

Co-administration of D-Pro^2-endomorphin-2 (50 and 100 pmol) at 1 or 5 min after i.t. injection produced a dose-dependent antagonism on inhibition of the paw withdrawal response by endomorphin-2 (Figure 1). The maximum antagonistic effect on endomorphin-2-induced antinociception was observed at 100 pmol of D-Pro^2-endomorphin-2, (Figure 2). The ID_{50} values for D-Pro^2-endomorphin-2 on inhibition of the paw withdrawal response by endomorphin-2 were 60.1 pmol and 70.0 pmol at 1 and 5 min after i.t. co-injection, respectively (Table 1). Antinociception induced by endomorphin-2 was unaffected by D-Pro^2-endomorphin-1 (0.03–1.0 pmol).

DAMGO, injected i.t. at a dose at 20 pmol, was antinociceptive in the paw withdrawal test. DAMGO-induced antinociception was antagonized significantly by D-Pro^2-endomorphin-1 (0.01–0.08 pmol) at 10 min post-co-injection, but not by D-Pro^2-endomorphin-2. The ID_{50} values for D-Pro^2-endomorphin-1 on DAMGO-induced antinociception were 0.022 pmol and 0.019 pmol at 5 and 10 min after i.t. co-injection, respectively.

Discussion

Spinal administration of endomorphin-1 and -2 at a dose of 5 nmol induced equipotent antinociception. The present results of i.t. administered endomorphins are in agreement with those of Stone *et al.* (1997) and Sakurada *et al.* (1999; 2000a) who reported that the antinociceptive effect of the endomorphins is short-lasting and is absent 15–20 min following i.t. injection, as assayed by the tail-flick test, paw withdrawal test and tail-pressure test. Endomorphins are

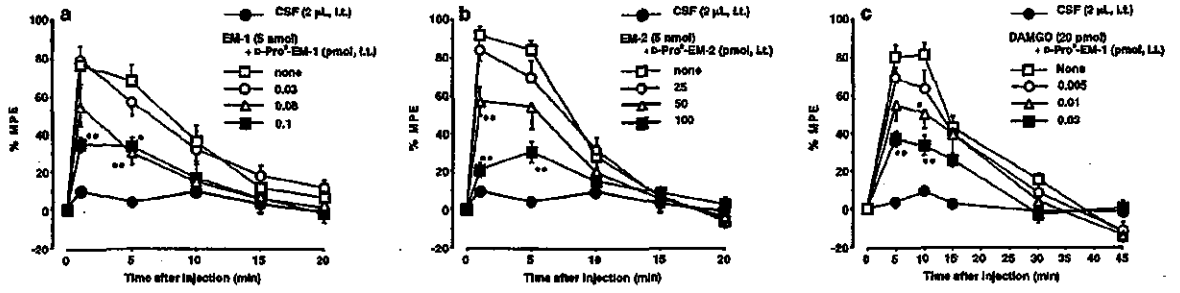

Figure 1 The time course of antagonistic effects of D-Pro^2-endomorphin-1 and D-Pro^2-endomorphin-2 on antinociception induced by i.t. endomorphin-1 (a), endomorphin-2 (b) and DAMGO (c) in the mouse paw withdrawal test. Endomorphins and DAMGO were co-administered i.t. with D-Pro^2-endomorphins. Each point in the time-course effect represents the mean ± s.e.mean of 10 mice. $^{**}P<0.01$, $^{*}P<0.05$, compared with each agonist alone. EM-1: endomorphin-1; EM-2: endomorphin-2.

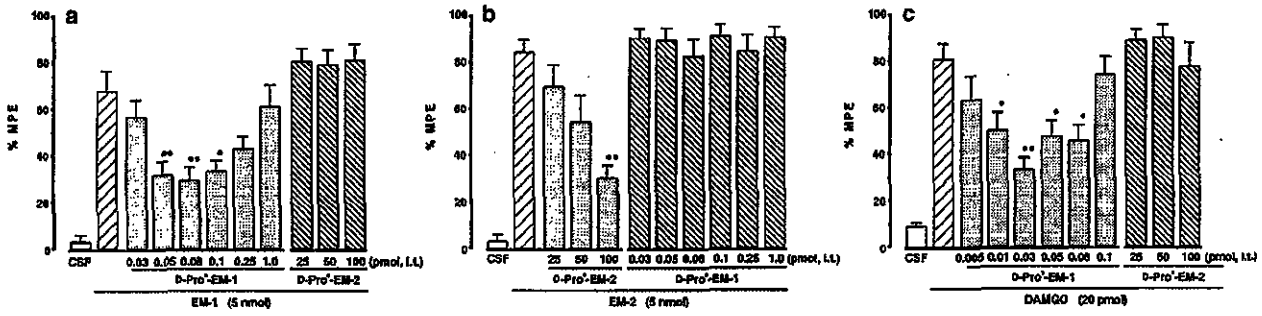

Figure 2 Effects of D-Pro^2-endomorphin-1 and D-Pro^2-endomorphin-2 on antinociception induced by i.t. endomorphin-1 (a), endomorphin-2 (b) and DAMGO (c) in the mouse paw withdrawal test. Each column represents the mean ± s.e.mean of 10 mice. Measurements were taken 5 and 10 min following i.t. endomorphins and DAMGO, respectively $^{**}P<0.01$, $^{*}P<0.05$, compared with each agonist alone. EM-1: endomorphin-1; EM-2: endomorphin-2.

Table 1 Antagonistic effect of D-Pro^2-endomorphin-1 and D-Pro^2-endomorphin-2 on antinociception induced by endomorphin-1, -2 and DAMGO in mice

Agonists (dose)	*Time after injection* (min)	ID_{50} (pmol) *D-Pro²-EM-1*	*D-Pro²-EM-2*
EM-1	1	0.13 (0.072–0.237)	–
(5 nmol)	5	0.058 (0.038–0.089)	–
EM-2	1	–	60.1 (39.95–90.41)
(5 nmol)	5	–	70.0 (40.4–121.0)
DAMGO	5	0.022 (0.01–0.046)	–
(20 pmol)	10	0.019 (0.008–0.044)	–

Values in parenthesis are 95% confidence limits. Each agonist was co-injected i.t. with D-Pro^2-endomorphin-1 or D-Pro^2-endomorphin-2. –, Significantly not antagonized; EM-1: endomorphin-1; EM-2: endomorphin-2.

small peptides that consist of only four amino acids, making them vulnerable to rapid degradation by peptidases. Dipeptidyl peptidase IV is a membrane bound serine proteinase proposed to be involved in the inactivation of endomorphins. Endomorphin-2-induced antinociception is modulated by the proteolytic enzyme, dipeptidyl peptidase IV such that dipeptidyl peptidase inhibitor itself, produces an opioid-sensitive antinociception, and enhances endomorphin-2-induced antinociception. An enzyme-resistant analogue of endomorphin-2, D-Pro^2-endomorphin-2 produces more potent and longer-lasting opioid sensitive antinociception after i.c.v. administration (Shane *et al.*, 1999). The diastereoisomer of endomorphin-1, D-Pro^2-endomorphin-1 possesses much lower potency than that of the parent peptide in the guinea-pig ileum assay, and is not an antagonist at either the μ- or κ-opioid receptors, as it is unable to shift the dose–response curve to either morphine or ethylketazocine (Paterlini *et al.*, 2000).

There is biochemical and pharmacological evidence supporting the existence of μ-opioid receptor subtypes, which are localized in spinal and supraspinal structures involved in the modulation of nociception (Wolozin & Pasternak, 1981; Moskowitz & Goodman, 1985). At least two μ-opioid receptor subtypes have been proposed; μ_1- and μ_2-. β-Funaltrexamine irreversibly antagonizes both μ_1- and μ_2-opioid receptors and inhibits both supraspinal and spinal antinociception, whereas naloxonazine selectively antagonizes the μ_1-opioid receptor. It is noteworthy that 35 mg kg^{-1} (s.c.) of naloxonazine is a reasonable dose to selectively block μ_1-opioid receptors in mice (Ling *et al.*, 1986). The antinoci-

ceptive effect of endomorphin-2 is completely blocked by pretreatment with naloxonazine at the dosage (35 mg kg^{-1} s.c.) which shows the selectivity to μ_1-opioid receptor in the paw withdrawal test, suggesting that endomorphin-2 may be a selective agonist for μ_1-opioid receptor. Pretreatment with naloxonazine at the dosage of 35 mg kg^{-1} (s.c.) does not block the antinociception induced by endomorphin-1 or DAMGO, whereas higher doses of naloxonazine (52.5 or 65.6 mg kg^{-1}, s.c.) significantly attenuate endomorphin-1 induced antinociception, indicating that at high dosage, naloxonazine may lose its selectivity for μ_1-opioid receptor (Sakurada *et al.*, 2000b). This means that endomorphin-1 or DAMGO can act as a predominantly μ_2-opioid receptor agonist and endomorphin-2 as a μ_1-opioid receptor agonist. Thus, endomorphin-1 has similarity of antinociception to DAMGO on lack of antagonism by naloxonazine. However, the selective μ_2-opioid antagonist has not yet been found.

We found in the present study that the antinociceptive effect of endomorphin-1 was inhibited by co-administration of D-Pro^2-endomorphin-1 but not by D-Pro^2-endomorphin-2. Antagonistic action of D-Pro^2-endomorphin-1 on endomorphin-1-induced antinociception reached a maximum effect at 0.08 pmol and declined with increases in doses. Similarly, the bell-shaped pattern in the dose–response of D-Pro^2-endomorphin-1 was observed in the case of DAMGO-induced antinociception. These results led to speculate that D-Pro^2-endomorphin-1 at higher doses may have an inhibitory action on endomorphin-1 degradation by peptidases. On the other hand, D-Pro^2-endomorphin-2 at a dose of 100 pmol significantly eliminated the antinociceptive activity produced by i.t. endomorphin-2 without affecting the antinociception of endomorphin-1 and DAMGO. The present study is the first to show that endomorphin analogues, D-Pro^2-endomorphin-1 and D-Pro^2-endomorphin-2 can distinguish the action of endomorphin-1 from that of endomorphin-2, suggesting possibility that D-Pro^2-endomorphin-1 may act as a μ_2-opioid receptor antagonist and D-Pro^2-endomorphin-2 as a μ_1-opioid receptor antagonist.

D-Pro^2-endomorphin-1 selectively blocked the antinociceptive effect of i.t. administered DAMGO, as well as endomorphin-1, whereas antinociception of Tyr-D-Arg-Phe-β-Ala (Sakurada *et al.*, 2000a), the selective μ_1-opioid receptor agonist was inhibited by co-administration of D-Pro^2-endomorphin-2 but not D-Pro^2-endomorphin-1 (unpublished data). These results also indicate that these two D-Pro^2-endomorphins may be a useful tool to discriminate between the antinociceptive effects of μ_1- and μ_2-opioid receptor agonists.

References

HORVATH, G., SZIKSZAY, M., TOMBOIY, C. & BENEDEK, G. (1999). Antinociceptive effects of intrathecal endomorphin-1 and -2 in rats. *Life Sci.*, **65**, 2635–2641.

LING, G.S.F., SIMANTOV, R., CLARK, J.A. & PASTERNAK, G.W. (1986). Naloxonazine action in vivo. *Eur. J. Pharmacol.*, **129**, 33–38.

MARTIN-SCHILD, S., GERALL, A.A., KASTIN, A.J. & ZADINA, J.E. (1999). Differential distribution of endomorphin 1- and endomorphin 2-like immunoreactivities in the CNS of the rodent. *J. Comp. Neurol.*, **405**, 450–471.

MOSKOWITZ, A.S. & GOODMAN, R.R. (1985). Autoradiographic distribution of MU_1 and MU_2 opioid binding in the mouse central nervous system. *Brain Res.*, **360**, 117–129.

OKADA, Y., FUKUMIZU, A., TAKAHASHI, M., SHIMIZU, Y., TSUDA, Y., YOKOI, T., BRYANT, S.D. & LAZARUS, L. (2000). Synthesis of stereoisomeric analogues of endomorphin-2, H-Tyr-Pro-Phe-Phe-NH_2, and examination of their opioid receptor binding activities and solution conformation. *Biochem. Biophys. Res. Commun.*, **276**, 7–11.

PATERLINI, M.G., AVITABILE, F., OSTROWSKI, B.G., FERGUSON, D.M. & PORTOGHESE, P.S. (2000). Stereochemical requirements for receptor recognition of the μ-opioid peptide endomorphin-1. *Biophys. J.*, **78**, 590–599.

PICK, C.G., PAUL, D. & PASTERNAK, G.W. (1991). Comparison of naloxonazine and β-funaltrexamine antagonism of μ_1 and μ_2 opioid actions. *Life Sci.*, **48**, 2005–2011.

PRZEWLOCKA, B., MIKA, J., LABUZ, D., TOTH, G. & PRZEWLOCKI, R. (1999). Spinal analgesic action of endomorphins in acute, inflammatory and neuropathic pain in rats. *Eur. J. Pharmacol.*, **367**, 189–196.

SAKURADA, S., HAYASHI, T., YUHKI, M., FUJIMURA, T., MURAYAMA, K., YONEZAWA, A., SAKURADA, C., TAKESHITA, M., ZADINA, J.E., KASTIN, A.J. & SAKURADA, T. (2000a). Differential antagonism of endomorphin-1 and endomorphin-2 spinal antinociception by naloxonazine and 3-methoxynaltrexone. *Brain Res.*, **881**, 1–8.

SAKURADA, S., TAKEDA, S., SATO, T., HAYASHI, T., YUKI, M., KUTSUWA, M., TAN-NO, K., SAKURADA, C., & SAKURADA, T. (2000b). Selective antagonism by naloxonazine of antinociception by Tyr-D-Arg-Phe-β-Ala, a novel dermorphin analogue with high affinity at μ-opioid receptors. *Eur. J. Pharmacol.*, **395**, 107–112.

SAKURADA, S., ZADINA, J.E., KASTIN, A.J., KATSUYAMA, S., FUJIMURA, T., MURAYAMA, K., YUKI, M., UEDA, H. & SAKURADA, T. (1999). Differential involvement of μ-opioid receptor subtypes in endomorphin-1- and -2 induced antinociception. *Eur. J. Pharmacol.*, **372**, 25–30.

SHANE, R., WILK, S. & BODNAR, R.J. (1999). Modulation of endomorphin-2-induced analgesia by dipeptidyl peptidase IV. *Brain Res.*, **815**, 278–286.

STONE, L.S., FAIRBANKS, C.A., LAUGHLIN, T.M., NGUYEN, H.O., BUSHY, T.M., WESSENDORF, M.W. & WILCOX, G.L. (1997). Spinal analgesic actions of the new endogenous opioid peptides endomorphin-1 and -2. *NeuroReport*, **8**, 3131–3135.

WOLOZIN, B.L. & PASTERNAK, G.W. (1981). Classification of multiple morphine and enkephalin binding sites in the central nervous system. *Proc. Natl. Acad. Sci. U.S.A.*, **78**, 6181–6185.

ZADINA, J.E., HACKLER, L., GE, L.J. & KASTIN, A.J. (1997). A potent and selective endogenous agonist for the μ-opiate receptor. *Nature*, **386**, 499–502.

(Received October 1, 2002
Accepted October 14, 2002)

Reiko Mineki
Hikari Taka
Tsutomu Fujimura
Mika Kikkawa
Noriko Shindo
Kimie Murayama

Division of Biochemical Analysis,
Central Laboratory of Medical Sciences,
Juntendo University School of Medicine,
Tokyo, Japan

In situ alkylation with acrylamide for identification of cysteinyl residues in proteins during one- and two-dimensional sodium dodecyl sulphate-polyacrylamide gel electrophoresis

Cysteinyl residues in proteins were alkylated with acrylamide during sodium dodecyl sulphate-polyacrylamide gel electrophoresis (SDS-PAGE) to yield a thioether derivative, cys-S-β-propionamide (PAM cys). The process was termed *in situ* alkylation with acrylamide. Using this method, the recovery of PAM-cys peptides from bovine serum albumin (BSA) was 88.6% at 10 picomol in one-dimensional (1-D) SDS-PAGE and 97.1% at 50 picomol in two-dimensional (2-D) SDS-PAGE. The coverage of tryptic peptide of BSA in 1-D and 2-D SDS-PAGE was 83.7% and 81.1%, respectively. The advantages of *in situ* alkylation with acrylamide were the following: (i) cysteinyl peptides were effectively derived in a single PAM cys and then proteins were precisely identified using databases; (ii) marked reduction of salts compared with post alkylation, *e.g.*, using carboxymethylamide (CAM), resulting in higher signal intensity and wider coverage of cysteinyl peptides from PAM cys, compared with those of CAM derivatives, in mass spectrometry peptide mapping; and (iii) shorter duration by excluding the processes of post alkylation and desalting before peptide mapping.

Keywords: Alkylation / Cysteinyl peptide / Peptide mapping / Sodium dodecyl sulphate-polyacrylamide gel electrophresis PRO 0289

1 Introduction

The combination of gel electrophoresis and mass spectrometry has developed into one of the most powerful tools for the identification of proteins in proteome analysis. Proteins isolated by 1-D or 2-D SDS-PAGE are in-gel digested with trypsin and identified by MS peptide mapping. However, many proteins contain free cysteinyl residues and disulphide bonds between inner- and intra-polypeptide chains to form protein tertiary structures. Thus, reduction and alkylation of cysteinyl residues in proteins is an important process before in-gel digestion. Using these methods, such peptides are effectively extracted from the gel, and could be subsequently analysed by PROWL (ProFound) and other software for peptide mapping, where the proteins are finally identified using published databases such as the NCBInr.

Correspondence: Prof. Kimie Murayama, Ph.D., Division of Biochemical Analysis, Central, Laboratory of Medical Sciences, Juntendo University School of Medicine, 2-1-1 Hongo, Bunkyo-ku, Tokyo 113-8421, Japan
E-mail: murayama@med.juntendo.ac.jp
Fax: +81-(3)-3818-6330

Abbreviations: CAM, iodoacetamide alkylation; **DTE**, dithioerythritol; **PAM**, propionamide alkylation; **PDA**, piperazine diacrylamide

Alkylation of protein cysteinyl residues in a gel slightly differs from that of proteins in a solution. Several reports described methods for alkylation of these residues in gels using iodoacetamide before or after SDS-PAGE [1–4]. In this regard, the results could be ambiguous when cysteinyl residues of proteins are alkylated on 1-D or 2-D SDS-PAGE using unpolymerized acrylamide and the process is not followed by thorough washing. Alkylation of cysteinyl residues in proteins with acrylamide during SDS-PAGE results in the formation of a thioether derivative, cys-S-β-propionamide (PAM cys).

Protein sequence analysis including PAM cys derivatives was reported by Brune in 1992 [5]. When proteins in mild alkaline solution are reacted with acrylamide, they form PAM cys on a phenylthiohydantoin (PTH) amino acid chromatogram. Yan *et al.* [6] reported the reactivity of alkylation of the SH group in cysteinyl residues and the epsilon amino groups in lysinyl residues based on the pH of the solution. They showed that alkylation of both residues occurred preferentially in alkaline pH compared with neutral pH and that lysine was not alkylated below pH 8.5. Sechi *et al.* [7] used alkylation of SH group before 1-D SDS-PAGE to improve the identification procedure by increasing the number of extracted peptides. In their method, 10 μL of 7 M acrylamide solution is added to 20 μL of the reduced sample and the mixture

 0173-0835/02/1212–1672 $17.50+.50/0

was allowed to stand in the dark for 1 h at room temperature. The coverage of alkylated cysteinyl residues in BSA was 30% by MALDI-TOF MS. On the other hand, Verrills *et al.* [8] used acrylamide and tributylphosphin (TBP) as a reducing agent before 2-D SDS-PAGE. Protein alkylation by acrylamide including its *N*-substituted derivatives, cross-linkers and immobilines was also reported by Hamadan *et al.* [9]. In general, the free cysteinyl residues easily convert the S-S bond bridges between intra- and inner-polypeptide chains in alkaline pH. In addition, the reactivity of alkylation of cysteinyl and lysinyl residues in proteins is pH- and time-dependent.

Alkylation of cysteinyl residues during electrophoresis is a side reaction with acrylamide. When proteins in a gel are alkylated with iodoacetamide (CAM) before peptide mapping, we have encountered a problem; the results of database searches for proteins using CAM derivatives are different from those using PAM derivatives. In the present study, we tried to unify the PAM cys and demonstrate the usefulness of alkylation using acrylamide during 1-D or 2-D SDS-PAGE, which was termed "*in situ* alkylation", for identification of cysteinyl residues of proteins, and to demonstrate that our technique is superior to alkylation using iodoacetamide.

2 Materials and Methods

2.1 Materials

Immobiline DryStrips at pH 3–10 (11 cm), IPG buffer, PlusOne silver staining kit and Coomassie Brilliant Blue (CBB-R350) were purchased from Amersham Biosciences (Uppsala, Sweden). Piperazine diacrylamide (PDA), ammonium persulphate (APS), TEMED and molecular marker proteins of broad range (molecular mass: 6.5–200 kDa) and precision (molecular mass: 10–250 kDa) on SDS-PAGE were obtained from Bio-Rad (Hercules, CA, USA). BSA was purchased from Sigma (St. Louis, MO, USA). Dithioerythritol (DTE) was purchased from Tokyokasei Kogyou (Tokyo, Japan) and acrylamide was purchased from Daichi Kagaku (Tokyo, Japan). Iodoacetamide was obtained from Wako Pure Chemicals (Osaka, Japan). Recombinant nonproteolytic trypsin was obtained from Promega (Madison, WI, USA), which was used for peptide mapping. All organic solvents were of HPLC grade, and all other chemicals at reagent grade were obtained from Wako or Sigma. Ultra purified water was obtained using a Milli-Q UV plus purification system (Millipore, Bedford, MA, USA) and used in all procedures.

2.2 Protein samples for comparison of alkylation on 1-D or 2-D SDS-PAGE

2.2.1 Standard proteins

To compare the protein profiles on 1-D SDS-PAGE with and without *in situ* alkylation of acrylamide, marker proteins at 0.67 μg each (10 pmol for BSA) were used. The band of BSA with acrylamide on 1-D SDS-PAGE was used for *in situ* alkylation experiment and the same band without acrylamide was used for alkylation with CAM after electrophoresis, which we termed post CAM. The recovered cysteinyl and tryptic peptides were compared in both methods. In addition, 50 pmol of BSA on 2-D SDS-PAGE was used to compare the alkylating behaviour of cysteinyl residues, which are usually available (termed batched (CAM and PAM), and *in situ* (PAM) electrophoresis in 2-D SDS-PAGE).

2.2.2 Mitochondrial fraction of mouse liver using one-step Nycodenz density gradient solution

Mitochondrial fractions were obtained by one-step separation of organelles from the mouse liver using freeze-thaw density gradient solution of Nycodenz, as reported recently by Murayama *et al.* [10]. The mitochondrial proteins with/without acrylamide were used for 1-D SDS-PAGE (1.5 μg for silver staining) and also those between batched and *in situ* alkylation with acrylamide were used for 2-D SDS-PAGE (90 μg for CBB staining).

2.3 1-D SDS-PAGE and alkylation of cysteinyl residues

The electrophoresis apparatus was obtained from Nihon Eido (Tokyo, Japan). The gel size was 130 × 130 × 1 mm (12 lanes) for 1-D SDS-PAGE. The concentrations of separating and stacking gels were 10% and 4% acrylamide containing 2.6% PDA. The gel was prepared, allowed to stand overnight for efficient polymerisation, and washed at 20 mA for 1 h. The samples were then loaded onto the gel. 1-D SDS-PAGE commenced at 5 mA for 1 h in order to concentrate proteins in the stacking gel and then at 10 mA *per* gel for 2 h. The running buffer consisted of 25 mM Tris, 19.2 mM glycine (pH 8.45) containing 0.1% SDS, according to Laemmli *et al.* [11]. Proteins in the gel were subsequently stained using the PlusOne silver nitrate reagent. In the final step, the protein profiles were determined using an image analyser, Master Scan (Scanalytics, Billerica, MA, USA).

2.3.1 *In situ* alkylation of acrylamide

The marker proteins at 0.67 μg each/10 μL pure water (BSA 10 pmol) and the mitochondria fraction (1.5 μg/10 μL) were added to 10 μL of the sample buffer (62.5 mM Tris-HCl, pH 8.5), containing 10% glycerol, 2% SDS, 0.1 M DTE and 0.0025% bromophenol blue. To ensure complete unfolding and reduction, the protein solution was incubated at 95°C for 3 min. After cooling of the reduced sample, 4.7 μL aliquot of 30% acrylamide stock solution (20 μmol) was added. Immediately after mixing, the samples were loaded on a stacking gel. The cysteinyl residues were alkylated with acrylamide during electrophoresis (*in situ* alkylation with acrylamide).

2.3.2 Post alkylation with iodoacetamide before in-gel digestion

Disulphide bridges of cysteinyl residues were reduced in the sample buffer containing 0.1 M DTE and loaded on the gel for 1-D SDS-PAGE without alkylation. After staining the proteins and cutting of bands, the cysteinyl residues were reduced again and alkylated with iodoacetamide using the method described by Arnott *et al.* [12] before gel digestion with trypsin. Excess alkylating reagent was washed out by 100 mM ammonium bicarbonate (pH 8.5).

2.4 2-D SDS-PAGE with alkylation of cysteinyl protein residues

For 1-D IEF of the sample, IPGphor strips (11 cm) at pH 3–10 were used. The samples were diluted by the IEF solution containing 9 M urea, 4% CHAPS, 65 mM DTE, 2% IPG buffer, pH 3–10, and bromophenol blue (BPB). Dried IPG strips were rehydrated overnight in the sample solution. Then, IEF was performed with the following steps; increasing voltage 30 V for 6 h, 60 V for 5–7 h, from 60 to 200 V for 1 h, from 200 to 500 V for 1 h, from 500 to 1000 V for 1 h, from 1000 to 8000 V for 1 h, and held at 8000 V for 2 h, *i.e.*, a total of 20.45 kVh.

Before 2-D SDS-PAGE, IPG strips were immersed in 5 mL solution containing 50 mM Tris-HCl (pH 8.5), 6 M urea, 30% glycerol, 2% SDS, 150 mM DTE, and 0.005% BPB for 10 min at room temperature in order to reduce the inner- and intra-disulphide bonds of cysteinyl residues. For the 2-D SDS-PAGE, we used a gel (168 × 160 × 190 × 1 mm; Nihon Eido), which was prepared as separating gel (10% T and 2.6% C) and for stacking gel (4% T, 2.6% C) similar to that for 1-D SDS-PAGE. The pre-run was performed at 40 mA for 45 min to remove the excess reagents and adjust gel condition. The IPG strip of reduced proteins was placed onto the stacking gel. At first, the 2-D SDS-PAGE commenced at 10 mA for 40 min in order to release proteins from the IPG strip and to stack those into the 2-D gel. Subsequently, the proteins were separated at 30 mA for 3.5 h. The proteins in the gels were stained by silver staining kit and CBB R-350 and profiled by image analysis software.

2.4.1 *In situ* alkylation with acrylamide

Three hundred μL of 300 mM acrylamide in equilibration buffer containing 50 mM Tris (pH 8.5), 6 M urea, 30% glycerol and 2% SDS was layered onto the stacking gel, and IPG strips treated with the reducing reagent were placed into the acrylamide solution.

2.4.2 Batched alkylation with acrylamide or iodoacetamide

In general, proteins reduced on the IPG strips were batched alkylated. After reduction of proteins, the IPG strip was alkylated with 5 mL of 300 mM acrylamide or iodoacetamide for 10 min at room temperature [13]. The IPG-strip was placed onto the surface of a stacking gel. Proteins with alkylated cysteinyl residues were released from the strip and stacked onto a gel of 2-D SDS-PAGE.

2.5 In-gel digestion with trypsin and extraction of peptides

In-gel digestion using trypsin was performed as described by Castellanos-Serra *et al.* with minor modification [14]. The bands/spots of proteins were excised with a razor blade and cut into 1 × 2 mm pieces. They were placed in a 0.5 mL microtube (Treff AG, Schweiz, Switzerland), washed with purified water for 10 min at 37°C (5 times), and destained with 50% acetonitrile in 100 mM ammonium bicarbonate (pH 8.5) and purified water, or until CBB faded out completely (3–4 times). The gel pieces were dehydrated by the addition of acetonitrile for 10 min at 37°C and dried in a vacuum centrifuge (Micro Vac MV-100; Tomy, Tokyo, Japan). They were rehydrated by adding 30–50 μL of trypsin at 10 ng/μL, dissolved in 100 mM ammonium bicarbonate at pH 8.5, and allowed to stand for 15–18 h at 37°C. Tryptic peptides were extracted with the following solutions (each 50 μL) for 10 min at 37°C: (i) 50% acetonitrile containing 0.1% TFA, (ii) a mixture of 15% isopropanol, 20% formic acid and 25% acetonitrile and 40% purified water; and (iii) 80% acetonitrile. The extracted solutions were pooled and evaporated to dryness in the vacuum centrifuge.

2.6 Mass spectrometric analysis to identify proteins

Peptide mapping was carried out using the API QSTAR Pulsar *i* hybrid mass spectrometer systems, which consisted of nano-ESI and TOF, (Applied Biosystems, Framingham, CA, USA). The QSTAR hybrid mass spectrometer was combined with a micro liquid chromatograph (Magic 2002; Michrom Bioresources, Aburn, CA, USA) with attached 0.2 mm id × 50 mm Magic C18 column. The solvent system consisted of (A) 0.1% formic acid, and (B) 0.1% formic acid/90% acetonitrile. The solvent program was 5%B for 5 min, gradient at 2.1% B/min for 45 min and 100%B for 5 min. The flow rate was 2.5 μL/min. MS conditions were as follows; ion spray voltage 3.8 kV; voltage for electron multiplier (CEM) 2200 V; and curtain gas nitrogen was at 10 psi. Identification of proteins was performed using PROWL (ProFound) and public domain databases (NCBI) available on the internet.

2.7 Blotting onto PVDF membrane and staining

Proteins on the gel were blotted onto Immobilon P^{SQ} using TE42 (Hoefer, Amersham Bioscience) at 50 V for 1.5 h in the Trans-blot buffer (10 mM CAPS, 10% methanol, pH 11.0), as described previously [15]. Proteins were visualised by staining with CBB R-350 for 5 min, followed by destaining with 50% methanol for 10 sec (5 times). The membrane was stored at 4°C until analysis.

2.8 *N*-terminal sequence analysis

The *N*-terminal amino acid sequence of lysozyme on the PVDF membrane of 1-D SDS-PAGE was performed by automated Edman degradation using a Hewlett Packard model G1005A (Palo Alto, CA, USA) protein sequencer attached to a HP1090 M liquid chromatograph as a PTH amino acid analyser. The program was a modified routine 3.1.

3 Results

3.1 Comparison of protein profiles of samples alkylated with/without acrylamide

Figure 1a shows 1-D SDS-PAGE profiles of the standard proteins. The 10% gel shows a better separation between bands 4 and 6. The M_r of band 4 (BSA, 35 Cys residues) and band 5 (ovalbumin, 6 Cys residues) seemed to be slightly larger on 1-D SDS-PAGE in samples alkylated with acrylamide than those without acrylamide treatment. The M_r of band 6 (carbonic anhydrase containing no cysteinyl residue) was similar with and without acrylamide. The protein profiles on 1-D SDS-PAGE did not change when excess acrylamide (*in situ* alkylation) was used. Figure 1b shows the 1-D SDS-PAGE patterns of mitochondria proteins fractionated mouse liver with and without acrylamide. Although the molecular masses of some bands around 37 kDa were slightly different, no artificial bands appeared at *in situ* alkylation.

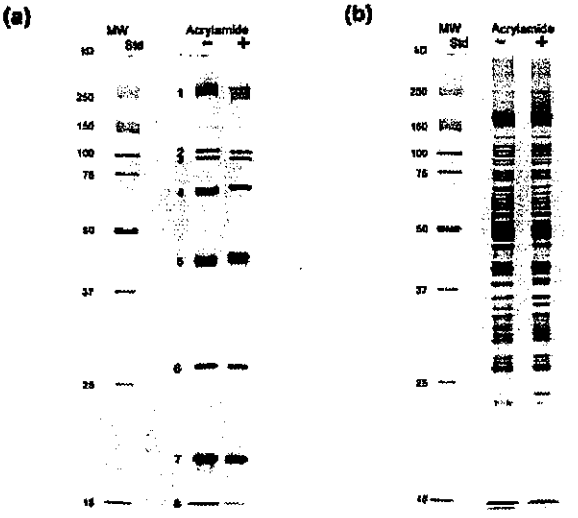

Figure 1. Alkylation with (+) or without (−) acrylamide of cysteinyl residues in proteins on 1-D SDS-PAGE. (a) Mixture of proteins: 1, myosin (200.0 kDa), 2, β-galactosidase (116.5 kDa), 3, phosphorylase β (97.4 kDa), 4, BSA (66.2 kDa), 5, ovalbumin (45.0 kDa), 6, carbonic anhydrase (31.0 kDa), 7, trypsin inhibitor (21.5 kDa) and 8, lysozyme (14.4 kDa). Fifty ng of each protein was loaded on 1-D SDS-PAGE with/without acrylamide. (b) Mouse mitochondria proteins (1.5 μg) with/without acrylamide. Proteins were stained using PlusOne silver nitrate.

3.2 Comparison of post and *in situ* alkylation of BSA

For peptide mapping, proteins separated on 1-D SDS-PAGE without acrylamide were digested with trypsin after reduction and alkylation by iodoacetamide (post alkylation). We compared the results of post and *in situ* alkylation on 1-D SDS-PAGE without desalting. Table 1 shows the process from solubilized proteins to peptide mapping for post and *in situ* alkylation.

In post alkylation with iodoacetamide, there was a high probability of induction of PAM-cys derivatives during electrophoresis because of side reaction with acrylamide, especially when we used a home-made gel. After electro-

Table 1. Comparison of 1-D SDS-PAGE using post alkylation and *in situ* alkylation

Step	Post alkylation with iodoacetamide	*In situ* alkylation with acrylamide
Solubilisation and reduction	yes	yes
Alkylation during electrophoresis	side reaction with unpolymerised acrylamide (PAM)	*in situ* alkylation (PAM)
Staining and destaining	yes	yes
Reduction	yes	no
Post-alkylation	iodoacetamide (CAM)	no
In-gel digestion with trypsin	yes	yes
Desalting	yes	no
Peptide mapping	yes	yes

phoresis, the protein bands were reduced again and alkylated by iodoacetamide. Excess salts were noted even though the gels were washed after alkylation with 100 mM bicarbonate without desalting (Fig. 1a). On the other hand, the cysteinyl residues of proteins processed by *in situ* alkylation were single derivatives and did not need any post alkylation and desalting steps. Thus, *in situ* alkylation was time consuming taking more than 100 min for post alkylation and about 10 min for desalting before MS analysis.

Figure 2 shows the results of MS mode TIC profiles for the tryptic peptides of BSA bands on 1-D SDS-PAGE using post (Fig. 2a) and *in situ* alkylation (Fig. 2b).

The insert chromatogram is the blank of reagents and gel for 1-D SDS-PAGE. Several unknown peaks including salts, were present in both chromatograms for 10 min even though the gel was washed out repeatedly with purified water, isopropanol, and acetonitrile (> 5 times) after iodoacetamide alkylation. The tryptic peptides were almost hidden within the peaks of unknown compounds. Figure 2b shows the chromatograms of blank and BSA *in situ* alkylated with acrylamide. The unknown peaks disappeared in both chromatograms compared with those of post alkylation. The unknown peaks resulted in not only delays of tryptic peptides on the retention times but also disturbed the mass spectrum, which showed typical detergent polymer ions such as + 44 (data not shown).

Since BSA has 1 cysteinyl and 17 cystinyl residues, the theoretical value of alkylated cysteinyl residues is 35. Table 2 compares BSA alkylated derivatives by post and *in situ* alkylation for 1-D SDS-PAGE. As expected, the post alkylation (CAM) was complex. Twenty-two cysteinyl residues completely and four residues partially converted to PAM cys during electrophoresis by unpolymerized acrylamide even though the gel was allowed to stand overnight and pre-run for 1 h. There were four CAM cys residues of which one at 513 Cys was completely converted and the other three at 264, 368 and 486 Cys were partially converted. There were three free cysteinyl residues at 391, 486 and 566. Cysteine at 486 was shared to free, CAM, PAM cysteinyl residues. Seven cysteinyl residues at 34, 53, 62, 90, 91, 167 and 168 could not be found. The recovery in CAM cys was only 11.4% while that of PAM cys was 74.3%. The recovery of free cysteinyl residues was also 8.6%. However, some of those shared different derivatives and the total recovery of cysteinyl residues was 80.0%, which covered 216 amino acid resi-

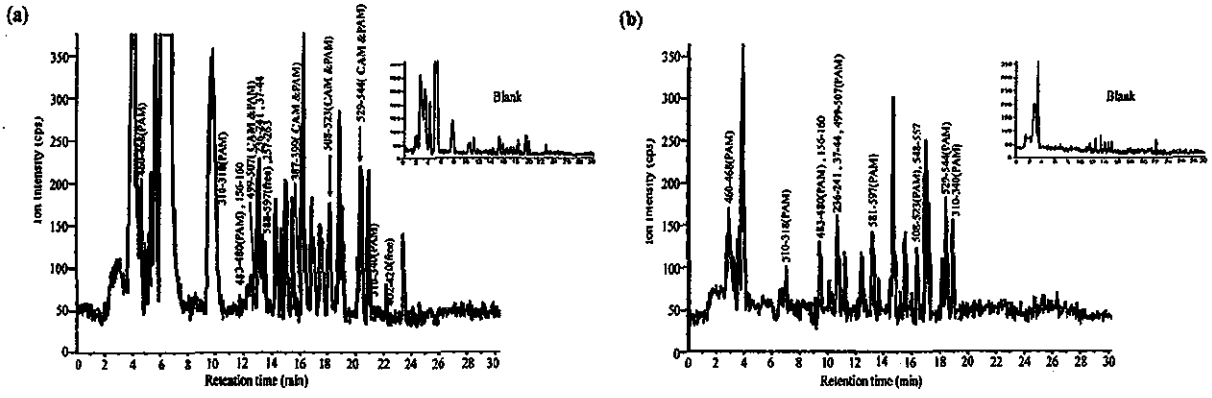

Figure 2. MS mode TIC profiles for the tryptic peptides of BSA by ESI-MS analysis (a) Post CAM cys, post alkylation with iodoacetamide (band 4 in Fig. 1a/ from the left lane) and (b) *in situ* PAM cys, *in situ* alkylation with acrylamide (band 4 in Fig. 1a/from the right lane). The sample used for MS analysis was 2 pmol (132 ng) of tryptic peptides of BSA.

Table 2. Comparison of alkylation between post CAM and *in situ* PAM for cysteinyl residues in BSA on 1-D SDS-PAGE

Item	Post CAM		*In situ* PAM	
a) Distribution of Cys derivatives				
	Cys No	Position	Cys No	Position
CAM-cys	1	513		–
CAM-cys and PAM-cys	2	264, 368		–
CAM-cys and PAM-cys and free cys	1	486		–
PAM-cys	22	others	31	others
PAM-cys and free cys	1	566		0
Free cys	1	391		0
Not found	7	34, 53, 62, 90, 91, 167, 168	4	34, 90, 91, 391
b) Recovery of Cys number[a)]				
	Cys No	Recovery	Cys No	Recovery
CAM-cys	4	11.4%		–
PAM-cys	26	74.3%	31	88.6%
Free cys	3	8.6%		–
Total	28	80.0%[a)]	31	88.6%
c) Coverage of amino acid residues				
	Residue	Coverage	Residue	Coverage
Cys peptides	216	37.0%	235	40.3%
Non-cys peptide	246	42.2%	253	43.4%
Total of tryptic peptide	462	79.2%	488	83.7%

The theoretical cysteine number of BSA is 35.

a) Value represents recovery of cysteinyl residues, which was calculated as the (number of the confirmed Cys/the theoretical Cys number) × 100.

dues (37.0%) of BSA, in post alkylation. The coverage of noncysteinyl peptides was 246 residues (42.2%) while the total coverage of the tryptic peptides for BSA by post alkylation was 79.2%.

On the other hand, the recovery of PAM cys by *in situ* alkylation was 88.6% and no free cysteinyl residues were noted. Only four residues at 34, 90, 91 and 391 Cys could not be detected (11.4%). The total coverage of homogenous derivative in tryptic peptides was 40.3% and that of noncysteinyl peptides was 43.4%. The total coverage of tryptic peptides for BSA by *in situ* alkylation was 83.7%. Although the coverage of tryptic peptides in both alkylation methods was not markedly different, the alkylated cysteinyl residues by *in situ* acrylamide were unified completely as PAM cys.

3.3 Extent of modification of alpha and epsilon amino groups of lysine at first residue of lysozyme by *in situ* alkylation with acrylamide

Acrylamide reacted with epsilon amino residue of lysine in the protein at alkaline pH at 8.45. The band of lysozyme separated by 1-D SDS-PAGE with *in situ* acrylamide, was blotted on a PVDF membrane and analysed by a protein sequencer.

Figure 3 shows 1–7 cycles of PTH chromatograms of 1-D SDS-PAGE separated lysozyme (10 pmol loaded in 1-D SDS-PAGE) after blotting on PVDF membrane. The PTH-lysine was 6.7 pmol in the first cycle, while the PTH-valine was 5.0 pmol in the second cycle. The *N*-terminal lysine was almost recovered at the first cycle even though acrylamide was used for alkylation of cysteinyl residues. At the sixth cycle, the recovery of the PTH-PAM cys was 4.4 pmol calculated by the colour value of the PTH-glycine, which was almost the same as that of PTH-PAM cys. The results indicate that *in situ* alkylation on 1-D SDS-PAGE is useful and convenient for protein sequencing and peptide mapping to identify proteins.

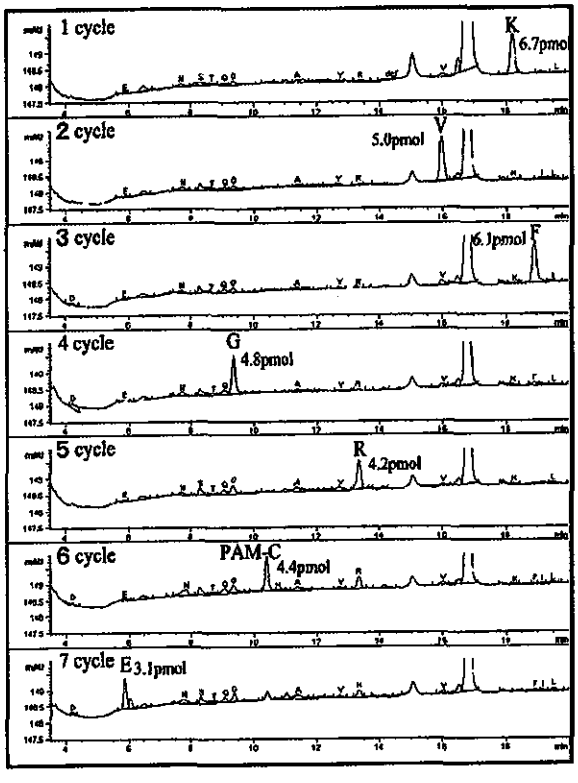

Figure 3. Protein sequencing for lysozyme *in situ* alkylated with acrylamide during 1-D SDS-PAGE. Lysozyme (10 pmol) was loaded on a gel for 1-D SDS-PAGE.

3.4 Comparison of batched and *in situ* alkylation on 2-D SDS-PAGE for MS

The process of 2-D SDS-PAGE includes reduction and batched alkylation of cysteinyl residues in proteins following 1-D IEF, prior to SDS gel electrophoresis (Table 3).

Table 3. The process of protein identification using batched and *in situ* alkylation

Step	Batched alkylation		*In situ* alkylation
	Iodoacetamide	Acrylamide	Acrylamide
1-D Electrofocusing			
Solubilisation	yes	yes	yes
Reduction (batched)	yes	yes	yes
Alkylation (batched)	iodoacetamide (CAM)	acrylamide (PAM)	no
2-D SDS-PAGE (pH 8.5)	side reaction with unpolymerised acrylamide (PAM)		*in situ* alkylation (PAM)
Staining and destaining	yes	yes	yes
In-gel digestion with trypsin	yes	yes	yes
Desalting	no	no	no
Peptide mapping	yes	yes	yes

When alkylation with iodoacetamide is only partially performed in this protocol, some of the free cysteinyl residues might be alkylated with unpolymerized acrylamide during SDS gel electrophoresis. Even though the same phenomenon occurs, the alkylated PAM cys derivative was of a single form in batched alkylation with acrylamide. We compared alkylation by batched iodoacetamide, batched acrylamide, and *in situ* acrylamide using BSA. Table 4 summarizes the differences in cysteinyl residues based on the method used for alkylation.

Batched iodoacetamide (CAM) induced 29 CAM cys (82.9%) and 3 partial CAM cys (8.6%). The total recovery of CAM cys was 91.4%. In batched PAM, 3 partial PAM cys were also observed at 475, 476 and 566 (8.6%). There were two free cysteinyl residues at 475 and 476 (5.7%) and three missing residues at 34, 90 and 91 (8.6%). The number of recovered cysteinyl residues was 32 (91.4%), which covered 243 amino acid residues (41.7%). The coverage of noncysteinyl peptides was 246 residues (42.2%) and the coverage of the total tryptic peptides was 83.9%. Batched acrylamide converted 32 PAM cys completely (91.4%) and 2 partially at 475 and 476 (5.7%). Two free cysteinyl residues were shared with PAM cys (5.7%). The recovery of PAM cys was 97.1%. The coverage of the cysteinyl and noncysteinyl peptides

Table 4. Comparison between batched and *in situ* alkylation for cysteinyl residues in BSA on 2-D SDS-PAGE

Item	Alkylation					
	Batched CAM		Batched PAM		*In situ* PAM	
a) Distribution of Cys derivatives	Cys No	Position	Cys No	Position	Cys No	Position
CAM-cys	29	others	–		–	
CAM-cys and PAM-cys	1	566	–		–	
CAM-cys and PAM-cys and free cys	2	475, 476	–		–	
PAM-cys	–		32	others	34	others
PAM-cys and free cys	–		2	475, 476	–	
Not found	3	34, 90, 91	1	34	1	34
b) Recovery of Cys number[a)]	Cys No	Recovery	Cys No	Recovery	Cys No	Recovery
CAM-cys	32	91.4%	–		–	
PAM-cys	3	8.6%	34	97.1%	34	97.1%
Free cys	2	5.7%	2	5.7%	–	
Total	32	91.4%[a)]	34	97.1%[a)]	34	97.1%
c) Coverage of amino acid residues	Residue	Coverage	Residue	Coverage	Residue	Coverage
Cys peptides	243	41.7%	255	43.7%	255	43.7%
Non-cys peptide	246	42.2%	234	40.1%	218	37.4%
Total of tryptic peptide	489	83.9%	489	83.9%	473	81.1%

The theoretical cysteine number of BSA is 35.

a) Value represents recovery of cysteinyl residues, which was calculated as the (number of the confirmed Cys/the theoretical Cys number) × 100.

was 43.7% (255 residues) and 40.1% (234 residues), respectively. Total coverage of tryptic peptides for BSA was 83.9%.

On the other hand, *in situ* alkylation with acrylamide showed 34 PAM cys (97.1%). Only one free cysteinyl at residue 34 was missing. The coverage of cysteinyl and noncysteinyl peptides was 43.7% (255 residues) and 37.7% (218 residues), respectively. The total coverage of tryptic peptides for BSA was 81.1%. *In situ* alkylation formed a single PAM cys even though the total coverage was lower than that of the other two methods. Since the recovery of the cysteinyl peptide was almost complete, in-gel digestion with trypsin was increased. Consequently, small peptides (< 4 residues) were missing but they were recovered in other methods by miscleaving with trypsin. The most hydrophobic tryptic peptide (M_r 2435.2, 21–41st residue) containing a free cysteinyl at residue 34 could not be confirmed on peptide mapping on 1-D or 2-D SDS-PAGE by any alkylation methods. The above results indicate that *in situ* alkylation provided the highest coverage of the cysteinyl peptides of BSA.

3.5 Comparison of protein profiles of mitochondria fractions of mouse liver on 2-D SDS-PAGE using batched and *in situ* alkylation with acrylamide

Finally, we compared the protein profiles of the mitochondria fraction of mouse liver using batched alkylation (Fig. 4a) and *in situ* alkylation with acrylamide (Fig. 4b). The two profiles were similar. Since some of the spots had different intensities in batched and *in situ* alkylation, they represent the same differences noted in protein profiles determined by the alkylation method (data not shown). We also compared the effect of alkylation method on representative spots, which are indicated by the solid arrows in Fig. 4. Since we compared the recovery of the batched and *in situ* PAM cys, glutamate dehydrogenase detected four PAM cys in both methods (66.7%). The spots were confirmed to be ATP synthase beta chain, glutamate dehydrogenase and catalase. Table 5 shows the recovery of PAM cys and the coverage of the amino acid residues in those in mouse mitochondria.

The recovery of the cysteinyl residues in catalase was also 60% in both methods. ATP synthetase beta chain did not contain any cysteinyl residues. The efficiency of *in situ* alkylation with acrylamide seemed to depend on the number and amounts of cysteinyl residues in proteins.

4 Discussion

In peptide mapping, we frequently encounter plural types of alkylated cysteine derivatives. They are PAM cys by unpolymerized acrylamide while the other forms are CAM based on the reagent used in the alkylation process. Since the presence of more than two derivatives from alkylated cysteinyl residues in proteins makes identification of proteins difficult using database searching, we performed *in situ* alkylation with acrylamide during 1-D or 2-D gel electrophoresis. In the first step of SDS-PAGE,

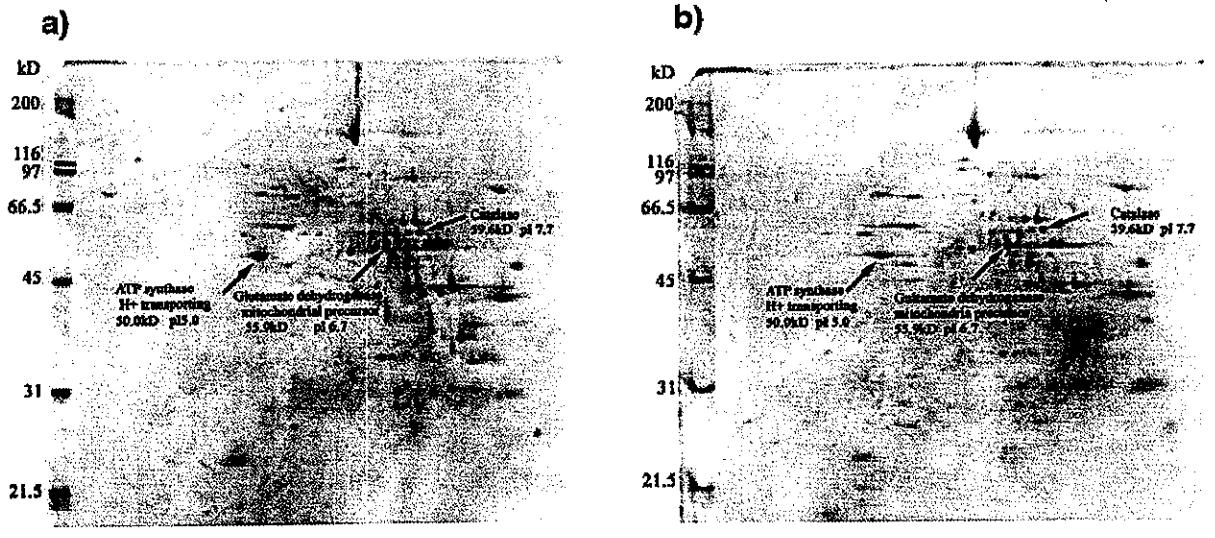

Figure 4. 2-D SDS electrophoresis protein profiles for mitochondria fraction of mouse liver organelles stained with Coomassie blue R-350 stain. (a) Batched alkylation with acrylamide (batched PAM cys); and (b) *in situ* alkylation with acrylamide (*in situ* PAM cys). The proteins (90 μg) were stained by CBB.

Table 5. Recovery of PAM Cys and coverage of amino acid residues in three proteins in mouse mitochondria

Item	Standard	Mouse liver mitochondria		
	BSA	ATP synthase beta chain	Glutamate dehydrogenase	Catalase
gi number	131907	114562	668027	115704
Mass	66433 Da	51710 Da	55912 Da	59634 Da
pI	5.60	4.95	6.71	7.72
a) Theoretical values				
AA residues	583	483	505	526
Cys residue	35	0	6	5
Cys percentage	6.0%	0%	1.2%	1.0%

b) Recovery of PAM cys number[a)]

	Cys No	Recovery (%)	Cys No	Recovery (%)	Cys No	Recovery (%)	Cys No	Recovery (%)
PAM cys	34	97.1	0	0	4	66.7	3	60.0
Free cys	0	0	0	0	0	0	0	0
Total	34	97.1	0	0	4	66.7	3	60.0

c) Coverage of amino acid residues

	Residue	Coverage (%)	Residue	Coverage (%)	Residue	Coverage (%)	Residue	Coverage (%)
Cys peptide	255	43.7	0	0	50	9.9	36	6.8
Non-cys peptide	218	37.4	336	69.6	336	66.5	339	64.4
Total peptide	473	81.1	336	69.6	386	76.4	375	71.2

a) BSA (2 pmol) and one third of tryptic peptides of each digested protein in mouse mitochondria (90 μg) from 2-D SDS-PAGE for LC-MS analysis.

proteins released from the IPG strip and cysteinyl residues were alkylated with acrylamide during electrophoresis. The process was termed in *situ* alkylation with acrylamide.

For 1-D SDS-PAGE, proteins were dissolved in the sample buffer at pH 6.8, which contained a detergent, reducing agent, and glycerol. They were denatured at 95°C for a few minutes before gel electrophoresis and running buffer at pH 8.45 was used according to Lammeli [11]. Thus, the cysteinyl and cystinyl residues of the protein were only reduced at the solubilisation step to produce free SH and then loaded on a gel at pH 8.4. A proportion of the free cysteinyl residues of the proteins was easily alkylated by unpolymerised acrylamide and also possibly cross-linked to other cysteinyl residues of the inner- or intra-polypeptide chains in alkaline pH during electrophoresis. In general, post alkylation with iodoacetamide is commonly used in 1-D SDS-PAGE as a CAM derivative (at 513). Some of the cysteinyl residues (at 264, 368, 486, 566) were common to CAM cys, PAM cys, and free cys, as shown in Table 2 and PAM cys derivatives were recovered at 74.3% (26 residues) before alkylation with iodoacetamide. This may be due to the use of self-prepared fresh gel plates. Since the unpolymerised acrylamide was progressively reduced in a ready-made gel, the PAM cys decreased more than the fresh gel (data not shown). However, the protein profiles of the fresh and old ready-made gels were different; the resolution and reproducibility of the protein bands decreased in older gels and the gel elasticity started to decrease. Accordingly, we always used home-made gels and these were allowed to stand for more than 15 h to obtain reproducible protein profiles.

Sechi *et al.* [7] reported that the presence or absence of cysteinyl residues in peptides is important for protein identification and that alkylation should be performed prior to electrophoresis to avoid the adventitious formation of acrylamide adducts during electrophoresis. In their study, homogenous alkylation was obtained with three different alkylating reagents (4-vinylpyridine, iodoacetamide and acrylamide). However, BSA at 2.5 pmol/10 μL was reduced by 10 μL of 5 mM DTT, which contained 0.9 M Tris-HCl (pH 8.45), 24% glycerol, and 8% SDS, at 100°C for 5 min and alkylated with acrylamide (70 μmol/10 μL) in the dark at room temperature for 1 h. The coverage of the tryptic peptides was 30% for 13

peptides by MALDI-TOF MS. Interestingly, the period of alkylation seemed to affect the recovery of cysteinyl peptides. Our results indicated that *in situ* alkylation was more effective than post alkylation for 1-D SDS-PAGE and allowed better mass analysis without desalting.

We also examined the effect of the method used for alkylation in 2-D SDS-PAGE, namely, batched and *in situ* alkylation using acrylamide as PAM cys and batched alkylation with iodoacetamide as CAM cys. Iodoacetamide was used since it is the most commonly used alkylating reagent on 1-D and 2-D SDS-PAGE for CAM cys. In batched CAM, recovery of CAM cys was incomplete; and reduction and alkylation were repeated after excising spots on 2-D SDS-PAGE [16]. On the other hand, in batched PAM, the recovery of PAM cys was 32 (91.4%) and the two PAM cys at 475 and 476 residues contained common free cysteinyl residues (5.7%). Thus, alkylation with acrylamide is more effective than that with iodoacetamide. The presence of the free cysteinyl residue in PAM cys did not pose a problem for protein identification.

The *in situ* alkylation of PAM cys allowed recovery of 34 (97.1%) and no free cysteinyl residue was found. Only a single cysteinyl residue at 34th was missing in this case. *In situ* alkylation has been performed during electrophoresis and provided the best coverage among the alkylation methods used in the present study.

BSA consists of a single polypeptide chain and includes 35 cysteinyl residues, including one free cysteinyl at 34 and 17 disulphide-bonded residues. It consists of three repeatable structures in addition to a helical structure. The highest molecular weight of hydrophobic tryptic peptide has a M_r 2435.2 (21–41st residue of BSA), which contains a free cysteinyl residue at the 34th, which could not be confirmed on 1-D or 2-D SDS-PAGE, irrespective of modification by any compound used in our study. Some of the missing cysteinyl residues were also buried in the α-helix and hydrophobic regions of BSA and accordingly, reduction and alkylation of these residues seemed to be difficult.

5 Concluding remarks

In this study we described *in situ* alkylation with acrylamide for cysteinyl residues in proteins during 1-D and 2-D SDS-PAGE. Acrylamide was added to the sample buffer and alkylation was performed during sample concentration and run in electrophoresis. After staining proteins, the bands or spots were directly digested with trypsin without any modification of cysteinyl residues again. Furthermore, the peptide mixtures were loaded on a column chromatograph-mass spectrometer without desalting to identify proteins. The method is a useful tool for proteomics.

This work was supported by a grant (#C-12670122) from the Ministry of Education, Culture, Sports, Science and Technology, Japan.

Received February 14, 2002

6 References

[1] Rabilloud, T., Valette, C., Laurence, J. T., *Electrophoresis* 1994, *15*, 1522–1558.

[2] Sanchez, J.-C., Rouge, V., Pitteur, M., Ravier, F. *et al.*, *Electrophoresis* 1997, *18*, 324–327.

[3] Sabounchi-Schutt, F., Astrom, J., Olsson. I., Eklund, A. *et al.*, *Electrophoresis* 2000, *21*, 3649–3656.

[4] Moritz, R. L., Eddes, J. S., Reid, G. E., Simpson, R. J., *Electrophoresis* 1996, *17*, 907–917.

[5] Brune, D. C., *Anal. Biochem.* 1992, *207*, 285–290.

[6] Yan, J. X., Kett, B. R., Herbert, B. R., Gooley, A. A., Packer, N. H., *J. Chromatogr. A* 1998, *813*, 187–200.

[7] Sechi, S., Chait, B. T., *Anal. Chem.* 1998, *70*, 5150–5158.

[8] Verrills, N. M., Harry, J. H., Walsh, B. J., Hains, P. G., Robinson, E. S., *Electrophoresis* 2000, *21*, 3810–3822.

[9] Hamadan, M., Bordini, E., Galvani, M., *Righetti, P. G., Electrophoresis* 2001, *22*, 1633–1644.

[10] Murayama, K., Fujimura, T., Morita, M., Shindo, N., *Electrophoresis* 2001, *22*, 2872–2880.

[11] Laemmli, U. K., *Nature* 1970, *227*, 680–685.

[12] Arnott, D., O'Connell, K. L., King, K. L., Stults, J. T., *Anal. Biochem.* 1998, *258*, 1–18.

[13] Yan, J. X., Sanche, J., Rouge, V., Williams, K. L., Hochstrasser, D. F., *Electrophoresis* 1999, *20*, 723–726.

[14] Castellanos-Serra, L., Proenza, W., Huerta, V., Moriz, R., Simpson, R., *Electrophoresis* 1999, *20*, 732–737.

[15] Matsudaira, P. T., *A Practical Guide to Protein and Peptide Purification for Microsequencing* Academic Press, pp. 53–60.

[16] Vallorani, L., Bernardini, F., Sacconi, C., Pierleon, R. *et al.*, *Electrophoresis* 2000, *21*, 3710–3716.

5. Adlkofer K, Martini R, Aguzzi A, et al. Hypermyelination and demyelinating peripheral neuropathy in PMP-22-deficient mice. Nat Genet 1995;11:274–280.
6. Kamholz J, Menichella D, Jani A, et al. Charcot-Marie-Tooth disease type 1: molecular pathogenesis to gene therapy. Brain 2000;123:222–233.
7. Amato AA, Gronseth GS, Callerame KJ, et al. Tomaculous neuropathy: a clinical and electrophysiological study in patients with and without 1.5-Mb deletions in chromosome 17p11.2. Muscle Nerve 1996;19:16–22.
8. Andersson PB, Yuen E, Parko K, et al. Electrodiagnostic features of hereditary neuropathy with liability to pressure palsies. Neurology 2000;54:40–44.
9. Infante J, Garcia A, Combarros O, et al. Diagnostic strategy for familial and sporadic cases of neuropathy associated with 17p12.2 deletion. Muscle Nerve 2001;24:1149–1155.
10. Mouton P, Tardieu S, Gouider R, et al. Spectrum of clinical and electrophysiologic features in HNPP patients with the 17p11.2 deletion. Neurology 1999;52:1440–1446.
11. Pareyson D, Scaioli V, Taroni F, et al. Phenotypic heterogeneity in hereditary neuropathy with liability to pressure palsies associated with chromosome 17p11.2–12 deletion. Neurology 1996;46:1133–1137.
12. Lewis RA, Sumner AJ, Shy ME, et al. Electrophysiological features of inherited demyelinating neuropathies: a reappraisal in the era of molecular diagnosis. Muscle Nerve 2000; 23:1472–1487.
13. Gouider R, LeGuern E, Gugenheim M, et al. Clinical, electrophysiologic, and molecular correlations in 13 families with hereditary neuropathy with liability to pressure palsies and a chromosome 17p11.2 deletion. Neurology 1995; 45:2018–2023.
14. Madrid R, Bradley WG. The pathology of neuropathies with focal thickening of the myelin sheath (tomaculous neuropathy), studies on the formation of the abnormal myelin sheath. J Neurol Sci 1975;25:415–448.
15. Yoshikawa H, Dyck PJ. Uncompacted inner myelin lamellae in inherited tendency to pressure palsy. J Neuropathol Exp Neurol 1991;50:649–657.
16. Dawson DM, Hallett M, Wilbourn AJ. Entrapment neuropathies. 3rd ed. Philadelphia: Lippincott–Raven, 1999.

Clinicopathological features of genetically confirmed Danon disease

K. Sugie, MD, PhD; A. Yamamoto, MD; K. Murayama, BS; S.J. Oh, MD; M. Takahashi, MD; M. Mora, MD; J.E. Riggs, MD; J. Colomer, MD; C. Iturriaga, MD; A. Meloni, MD; C. Lamperti, MD; S. Saitoh, MD, PhD; E. Byrne, MD, DSc; S. DiMauro, MD; I. Nonaka, MD, PhD; M. Hirano, MD; and I. Nishino, MD, PhD

Abstract—*Background*: Danon disease is due to primary deficiency of lysosome-associated membrane protein-2. *Objective*: To define the clinicopathologic features of Danon disease. *Methods*: The features of 20 affected men and 18 affected women in 13 families with genetically confirmed Danon disease were reviewed. *Results*: All patients had cardiomyopathy, 18 of 20 male patients (90%) and 6 of 18 female patients (33%) had skeletal myopathy, and 14 of 20 male patients (70%) and one of 18 female patients (6%) had mental retardation. Men were affected before age 20 years whereas most affected women developed cardiomyopathy in adulthood. Muscle histology revealed basophilic vacuoles that contain acid phosphatase–positive material within membranes that lack lysosome-associated membrane protein-2. Heart transplantation is the most effective treatment for the otherwise lethal cardiomyopathy. *Conclusions*: Danon disease is an X-linked dominant multisystem disorder affecting predominantly cardiac and skeletal muscles.

NEUROLOGY 2002;58:1773–1778

Danon disease, an X-linked cardioskeletal myopathy originally reported as "lysosomal glycogen storage disease with normal acid maltase,"[1] is caused by primary deficiency of lysosome-associated membrane protein-2 (LAMP-2), a major lysosomal membrane protein.[2] Together with its paralogous counterpart LAMP-1, LAMP-2 is a highly glycosylated protein coating the inner side of the lysosomal membrane. The *LAMP-2* gene is located on Xq24.[3] LAMP-2 is thought to protect the lysosomal membrane from proteolytic enzymes within lysosomes and to act as a receptor for proteins to be imported into lysosomes.[4] However, the precise functional role of LAMP-2 is still controversial.

Danon disease is characterized clinically by the triad of cardiomyopathy, myopathy, and mental re-

From the Departments of Ultrastructural Research (Drs. Sugie, Yamamoto, Nonaka, and Nishino, and K. Murayama) and Neuromuscular Research (Dr. Nishino), National Institute of Neuroscience, National Center of Neurology and Psychiatry, Kodaira, Tokyo, Japan; the Department of Neurology (Dr. Sugie), Nara Medical University, Kashihara, Nara, Japan; the Department of Neurology (Dr. Oh), University of Alabama at Birmingham; the Department of Pediatrics (Drs. Takahashi and Saitoh), Hokkaido University, Sapporo, Hokkaido, Japan; the Department of Neuromuscular Diseases (Dr. Mora), National Neurological Institute "C. Besta," Milan, Italy; the Department of Neurology (Dr. Riggs), West Virginia University, Morgantown; Hospital Sant Joan de Déu (Drs. Colomer and Iturriaga), Barcelona, Spain; the Department of Pediatrics (Dr. Meloni), University of Cagliari, Italy; the Department of Clinical Neurosciences (Dr. Byrne), St. Vincent's Hospital, Fitzroy, Australia; and the Department of Neurology (Drs. Lamperti, DiMauro, and Hirano), Columbia University, New York, NY.

Supported in part by the Research Grant (11B-1) for Nervous and Mental Disorders from the Ministry of Health and Welfare.

Received November 5, 2001. Accepted in final form March 14, 2002.

Address correspondence and reprint requests to Dr. Ichizo Nishino, Department of Neuromuscular Research, National Institute of Neuroscience, National Center of Neurology and Psychiatry, 4-1-1 Ogawahigashi-cho, Kodaira, Tokyo 187-8502, Japan; e-mail: nishino@ncnp.go.jp

Table 1 Summary of 13 families with Danon disease

Family	Ethnic background	Site of *LAMP-2* gene mutation	Affected men	Affected women	Study
1	Japanese	E9b	Proband, 1 cousin	Mother, 1 sister	9, 12
2	Japanese	E4	Proband	—	16
3	Japanese	I6*	Proband	Mother	3, 11
4	Italian	E8	Proband, 1 nephew	Mother, 1 sister	10
5	Afro-American	E8	Proband	Mother, 1 grandmother	
6	Japanese	I5	Proband	—	
7	Afro-American	I5	Proband	Mother, 2 sisters	7
8	Anglo-Saxon	I5	Proband, 1 brother	Mother	4
9	Japanese	I5/E6 junction	Proband	Mother	
10	Greek	E1	Proband, 2 cousins	Mother, 1 aunt	14
11	Japanese	E7	Proband	1 Sister	
12	Spanish	E2	Proband, 2 cousins	Mother, 1 grandmother, 1 aunt	
13	Italian	E4	Proband	—	

* Exon skipping mutation.

tardation.[1,5,6] Muscle biopsy reveals small autophagic vacuoles in muscle fibers. Some of these vacuoles have features of plasma membrane.[7] Diagnosis had been based on these clinical and histologic features in addition to normal acid maltase activity in skeletal muscle. However, disorders reported as "lysosomal glycogen storage disease with normal acid maltase" are genetically heterogeneous. In fact, two patients reported to have an infantile form of Danon disease did not have LAMP-2 deficiency.[8]

To better delineate the clinicopathologic features of Danon disease, we studied 38 patients from 13 families with genetically confirmed Danon disease.

Materials and methods. *Patients.* We reviewed the clinicopathologic features of 20 affected men and 18 affected women from 13 families with genetically confirmed Danon disease. Immunohistochemistry, Western blot analyses, or both confirmed LAMP-2 deficiency in all specimens. Clinical manifestations of seven of the 13 families were reported previously.[1,5,6,9-14] Statistical values are expressed as mean ± SD.

Sequence analysis. The open reading frame of the *LAMP-2* gene consists of nine exons. Human exon 9 exists in two forms, exon 9a and 9b, that are alternatively spliced and processed into two isoforms, *LAMP-2a* and *LAMP-2b*.[15] We sequenced the entire coding region, including both exons 9a and 9b, and the exon/intron junctions of the *LAMP-2* gene as described.[2]

Muscle biopsy. Muscle biopsy was performed in all probands. Biopsy specimens were either frozen in liquid nitrogen–cooled isopentane for histochemistry or fixed with glutaraldehyde for electron microscopy. Transverse serial frozen sections of 10-μm thickness were stained with hematoxylin and eosin, modified Gomori trichrome, and a battery of histochemical methods.

In addition, we performed indirect immunofluorescence staining on 6-μm cryosections of muscle using mouse monoclonal antibodies according to methods described previously.[16] These sections were incubated at 37 °C for 2 hours with the primary mouse IgG antibodies against LAMP-2 (H4B4, Developmental Studies Hybridoma Bank, Iowa City, IA), the C-terminal of dystrophin (NCL-DYS2, Novocastra, Newcastle Upon Tyne, UK), laminin α2 (NCL-MEROSIN, Novocastra), and α-sarcoglycan (NCL-α-SARC, Novocastra). They were subsequently incubated at 37 °C for 1 hour with a secondary antibody fluorescein isothiocyanate–labeled goat F(ab')2 antimouse IgG (M102, Leinco Technology, St. Louis, MO). All sections were examined by fluorescence microscopy. Control specimens were obtained from 10 patients with morphologically normal muscle.

For electron microscopy, biopsy specimens were fixed in buffered 2% isotonic glutaraldehyde at pH 7.4, postfixed in osmium tetroxide, and embedded in epoxide resin. Ultrathin sections were stained with uranyl acetate and lead nitrate and examined with an *H-7000* electron microscope (Hitachi). When sufficient tissues was available, we also performed Western blot analysis.

Results. *LAMP-2 gene mutations.* We identified *LAMP-2* mutations in all of the probands and affected family members from whom samples were available (table 1).[5] All mutations were either nonsense or frame-shift mutations that are predicted to cause truncation of the protein, except for the exon 6 skipping mutation in Family 3.[5]

Protein analysis. On immunohistochemical analysis, LAMP-2 staining was completely absent in muscle of the probands. By Western blot analysis, LAMP-2 was undetectable except for the proband in Family 1 who showed a small amount of LAMP-2 protein, as reported previously.[5]

Clinical features. The clinical features in 20 male patients with Danon disease are summarized in table 2. All 13 probands were male. The two most common features were cardiomyopathy and myopathy; mental retardation was present in 14 of the 20 male patients.

Ages at onset in the 20 male patients varied from 10 months to 19 years. Onset may be earlier but may go undetected because of the subacute nature and slow pro-